การสังเคราะห์และศึกษาลักษณะอนุภาคนาโนของ ทองแดง-สังกะสี โดยวิธีการอาร์คแบบจุ่ม

นางสาวหนึ่งฤทัย ปานอุทัย

วิทยานิพนธ์นี้เป็นส่วนหนึ่งของการศึกษาตามหลักสูตรปริญญาวิศวกรรมศาสตรมหาบัณฑิต
สาขาวิชาวิศวกรรมเคมี ภาควิชาวิศวกรรมเคมี
คณะวิศวกรรมศาสตร์ จุฬาลงกรณ์มหาวิทยาลัย
ปีการศึกษา 2556

SYNTHESIS AND CHARACTERIZATION OF Cu-Zn NANOPARTICLES BY SUBMERGED ARC DISCHARGE METHOD

Miss Neungruthai Panuthai

A Thesis Submitted in Partial Fulfillment of the Requirements
for the Degree of Master of Engineering Program in Chemical Engineering
Department of Chemical Engineering
Faculty of Engineering
Chulalongkorn University
Academic Year 2013

Thesis Title	SYNTHESIS AND CHARACTERIZATION OF Cu-Zn NANOPATRICLES BY SUBMERGED ARC DISCHARGE METHOD
By	Miss Neungruthai Panuthai
Field of Study	Chemical Engineering
Thesis Advisor	Assistant Professor Soorathep Kheawhom, Ph.D.

Accepted by the Faculty of Engineering, Chulalongkorn University in Partial Fulfillment of the Requirements for the Master's Degree

.....Dean of the Faculty of Engineering

(Professor Bundhit Eua-arporn, Ph.D.)

THESIS COMMITTEE

.....Chairman

(Professor Piyasan Prasertdam, Dr.Ing.)

.....Thesis Advisor

(Assistant Professor Soorathep Kheawhom, Ph.D.)

.....Examiner

(Associate Professor Anongnat Somwangthanaroj, Ph.D.)

.....External Examiner

(Assistant Professor Sirirat Wacharawichanant, D.Eng.)

หนึ่งฤทัย ปานอุทัย : การสังเคราะห์และศึกษาลักษณะอนุภาคนาโนของ ทองแดง-สังกะสี โดยวิธีการอาร์คแบบจุ่ม. (SYNTHESIS AND CHARACTERIZATION OF Cu-Zn NANOPARTICLES BY SUBMERGED ARC DISCHARGE METHOD)
อ.ที่ปรึกษาวิทยานิพนธ์หลัก: ผศ. ดร.สุรเทพ เขียวหอม, 50 หน้า.

วิทยานิพนธ์เล่มนี้เสนอการสังเคราะห์อนุภาคนาโนของ ทองแดง-สังกะสี โดยวิธีการอาร์คแบบจุ่มของลวดที่มีทองแดง 90 %wt และสังกะสี 10 %wt ในความดันบรรยากาศ และของเหลวที่เป็นฉนวนไฟฟ้าทั้ง 4 ชนิด ได้แก่ น้ำปราศจากไอออน เอทานอล เอทีลีนไกลคอล และไดเอทาโนลามีน ถูกใช้ในระบบการสังเคราะห์ด้วยการอาร์คแบบจุ่ม ขนาดและลักษณะทางสัณฐานวิทยาของอนุภาคที่สังเคราะห์ได้ถูกวิเคราะห์โดย กล้องจุลทรรศน์อิเล็กตรอนแบบส่องผ่าน (TEM) กล้องจุลทรรศน์อิเล็กตรอนแบบส่องกราด (SEM) และเครื่องวิเคราะห์การเลี้ยวเบนของรังสีเอกซ์ (XRD) ผลของ XRD แสดงว่าอนุภาคนาโนที่สังเคราะห์ในน้ำกลั่นปราศจากไอออน เอทานอล เอทีลีนไกลคอล ประกอบด้วยอนุภาคของ ทองแดง-สังกะสี และอนุภาคออกไซด์ของสังกะสี (ZnO) ซึ่งถูกสร้างจากไอออนอิสระของออกซิเจนในระหว่างการสลายตัวของของเหลวที่ใช้ ตรงข้ามกับผลของ XRD ของอนุภาคนาโนที่สังเคราะห์ในไดเอทาโนลามีนที่แสดงเพียงพีคอัลลอยด์ของ ทองแดง-สังกะสี เท่านั้น ดังนั้นการเกิดซิงค์ออกไซด์สามารถป้องกันโดยการใช้ไดเอทาโนลามีนเป็นของเหลวฉนวนไฟฟ้า ขนาดของอนุภาคที่ได้จากการสังเคราะห์ในไดเอทาโนลามีนเป็น 10 ถึง 40 นาโนเมตร อนุภาคนาโนที่สังเคราะห์ได้ในไดเอทาโนลามีนถูกผสมกับแอมโมเนียน้ำปราศจากไอออน และซิลเวอร์ออกไซด์เพื่อเตรียมหมึกนำไฟฟ้า หมึกดังกล่าวถูกปาดลงบนแผ่นฟิล์ม PET ค่าความต้านทานของแผ่นฟิล์มถูกวัดด้วยเครื่องมิเตอร์ LCR และเมื่ออบแผ่นแพทเทิลในอากาศที่ 150 องศาเซลเซียล เป็นเวลา 60 นาที ค่าความต้านทานของแผ่นฟิล์มจะน้อยสุดเป็น 190 ไมโครโอห์มเซนติเมตร

ภาควิชา วิศวกรรมเคมี ลายมือชื่อนิสิต .....

สาขาวิชา วิศวกรรมเคมี ลายมือชื่อ อ.ที่ปรึกษาวิทยานิพนธ์หลัก .....

ปีการศึกษา 2556

5570438621 : MAJOR CHEMICAL ENGINEERING
KEYWORDS: NANOPARTICLE / SUBMERGED ARC DISCHARGE / CU-ZN

NEUNGRUTHAI PANUTHAI: SYNTHESIS AND CHARACTERIZATION OF CU-ZN NANOPARTICLES BY SUBMERGED ARC DISCHARGE METHOD.
ADVISOR: ASST. PROF. SOORATHEP KHEAWHOM, Ph.D., 50 pp.

This research presents Cu-Zn nanoparticles synthesis by submerged arc discharge of brass rod (Cu 90%wt/Zn 10%wt) in an ambient atmospheric pressure. Four types of dielectric liquid including deionized water, ethanol, ethylene glycol and diethanolamine were used in arc-submerged nanoparticles synthesis system. The particle size, microstructure and morphology of nanoparticles synthesized were characterized via transmission electron microscopy (TEM), Scanning electron microscope (SEM) and X-ray diffraction (XRD), respectively. The XRD patterns show that the nanoparticles synthesized in deionized water, ethanol and ethylene glycol consist of Cu-Zn alloy and zinc oxide. Zinc oxide was formed by oxygen free radicals during decomposition of the dielectric liquids used. In contrast, the XRD pattern of the nanoparticles synthesized in diethanolamine show peaks of only Cu-Zn alloy. Thus, formation of zinc oxide can be prevented by using diethanolamine as dielectric liquid. The nanoparticles synthesized were spherical with size ranging from 10 nm to 40 nm. The nanoparticles synthesized in diethanolamine were mixed with ammonia, deionized water and silver oxide to prepare a conductive ink. The conductive ink formulated was screen printed on polyethylene terephthalate (PET) substrate. The resistivities of the patterns obtained were then measured by LCR meter. By baking the printed pattern in air at 150 $^{\circ}$C for 60 min, the lowest volume resistivity of the printed pattern is 190 $\mu\Omega$.cm.

Department: Chemical Engineering Student's Signature .....
Field of Study: Chemical Engineering Advisor's Signature .....
Academic Year: 2013

ACKNOWLEDGEMENTS

This research received many graceful stimulations and suggestions by Asst. Prof. Soorathep Kheawhom, Prof. Piyasan Prasertdam, Assoc. Prof. Anongnat Somwangthanaroj, Assoc. Prof. Supakanok Thongyai and Asst. Prof. Sirirat Wacharawichanant. Author also acknowledges partially support from the Mektec Manufacturing Corporation (Thailand) Ltd. for financial supporting with materials and technician equipments and finally, author would like to thanks for support by the Ratchadaphisek Somphot Endowment Fund of Chulalongkorn University.

CONTENTS

Page

THAI ABSTRACT iv
ENGLISH ABSTRACT v
ACKNOWLEDGEMENTS vi
CONTENTS vii
LIST OF TABLES x
LIST OF FIGURES xi
CHAPTER I 1
INTRODUCTION 1
1.1 Background and motivation 1
1.2 Objective of the research 2
1.3 Scope of the research 2
1.4 Expected benefits 3
CHAPTER II 4
LITERATURE REVIEW 4
2.1 Synthesis of metal nanoparticles by arc discharge method 4
2.1.1 Silver 4
2.1.2 Copper 5
2.1.3 Alloy of copper 5
2.1 Synthesis of Cu-Zn alloy nanoparticles by arc discharge method 6
2.2 Sintering of metal conductive ink for flexible electronic 7
CHAPTER III 9
FUNDAAMENTALS 9
3.1 Conductive ink technology 9
3.2 Plasma nanoscience 9
3.3 Brass properties 11
3.4 Nanometals 12
3.5 Ink binder 13

Page

3.6 Screen printing 14
3.6.1 Flexible substrates 14
3.6.2 Screen printing method 15
3.7 Sintering process 16
3.7.1 Sintering mechanisms 16
3.7.2 Nanomaterial Sintering 17
CHAPTER IV 20
EXPERIMENTAL 20
4.1 Materials 20
4.2 Study of process of the nano Cu-Zn conductive ink 20
4.2.1 Synthesis of Cu-Zn nanoparticles by arc discharge method 20
4.2.2 Effect of dielectric liquid and storage 21
4.3 Preparation of binder 22
4.4 Preparation of Cu-Zn conductive ink 22
4.5 Study of conductive pattern 23
4.5.1 Screen printing 23
4.5.2 Effect of sintering 23
4.6 Characterizations 24
CHAPTER V 25
RESULTS AND DISCUSSIONS 25
5.1 Synthesis, characterization and stability of Cu-Zn nanoparticles by arc discharge method in different dielectric liquid 25
5.2 Thermal properties of the nano Cu-Zn ink 31
5.3 Sintering and conductivity of the Cu-Zn pattern 34
CHAPTER VI 43
CONCLUSIONS 43
6.1 Summary of Results 43
6.2 Recommendations 44

Page

REFERENCES 45
APPENDIX 48
VITA 50

LIST OF TABLES

Table **Page**

3.1 Physical properties of plastic material for substrates..... 12
4.1 The process parameter to investigate effect of dielectric liquid..... 20
4.2 The experimental design of sintering under different gas..... 22
5.1 Summary of volume resistivity of the printed film under various annealing conditions..... 42

LIST OF FIGURES

Figure **Page**

2.1 Schematic diagrams showing the arc discharge process in liquid..... 4
2.2 Comparison of theXRDpatterns the golden nanobrass and ZnO products obtained after the arc discharge treatments in different media..... 6
2.3 The SEM image of Cu-Zn nanoparticle synthesized at arc current of 300 A and 1 atm of Ar..... 7
2.4 Variations of resistivity and FE-SEM images of surface copper film after annealing at various conditions..... 8
3.1 Schematics of the interelectrod gap..... 10
3.2 Nanoparticles growth in plasma..... 11
3.3 Structure formula of polyethylene terphthalate..... 15
3.4 Screen printing concept..... 16
3.5 Illustration of agglomeration 18
3.6 Illustration of densifying and non-densifying diffusions and their sintering results..... 19
4.1 The schematic diagram of the Arc discharge system..... 21
4.2 Procedure of Cu-Zn conductive ink preparation..... 22
4.3 Two point probe pattern..... 23
5.1 SEM images of nanoparticles synthesized in different dielectric liquids..... 26
5.2 TEM images of nanoparticles synthesized in different dielectric liquids..... 27
5.3 X-ray diffraction patterns of nanoparticles synthesized in different dielectric liquids..... 29
5.4 X-ray diffraction patterns of Cu-Zn nanoparticles after storing in diethanolamine for 2 month and 6 month..... 29
5.5 SEM/EDX images of nanoparticles synthesized in diethanolamine..... 30
5.6 SEM/EDX patterns of Cu-Zn nanoparticles synthesized in diethanolamine..... 30
5.7 TGA/DTA curve of the nano Cu-Zn ink in air atmosphere..... 31

Figure **Page**

5.8 TGA-DTA curve of the nano Cu-Zn ink after silver complex binderadding..... 32
5.9 Derivative of heat flow curve of the nano Cu-Zn ink before and after silver complex binder adding..... 33
5.10 X-ray diffraction pattern of the printed film using nano Cu-Zn ink and then were sintered in air at 150 ℃ for 15 - 60 min..... 34
5.11 X-ray diffraction pattern of the printed film using nano Cu-Zn ink and then were heated in air at 100 ℃ for 30 min before sintering under 2% H_2-N_2 gas at 150 ℃ for 15 - 60 min..... 35
5.12 The screen printed pattern using nano Cu-Zn ink was coated on PET film after sintering at 150 ℃ in air atmosphere for 15 - 60 min..... 36
5.13 SEM and cross-section images of the printed film using nano Cu-Zn ink and then were sintered in air at 150 ℃ for 15 - 60 min..... 37
5.14 SEM and cross-section images of the printed film using nano Cu-Zn ink and then were heated in air at 100 ℃ for 30 min before sintering under 2% H_2-N_2 gas at 150 ℃ for 15 - 60 min..... 38
5.15 Fracture of printed films was sintered for 45 min and 60 min..... 39
5.16 TGA/DTA curve of the Cu-Zn printed film was cured at 150 ℃ in air atmosphere..... 40

CHAPTER I

INTRODUCTION

1.1 Background and motivation

Printed and flexible electronic technology has been successively developed [1, 2]. Conductive ink widely used is based on silver nanoparticles because silver has highest electrical conductivity at room temperature. Moreover, silver oxide has considerable conductivity.

Copper is one alternate metal that can replace silver because it has lower cost. Moreover, its conductivity is the second highest of any metals. However, copper-rich lattice necessary requires stabilization [3] especially in nano form. Copper nanoparticle is prune to form oxide in atmospheric condition, and copper oxide is not electrically conductive. Copper oxide requires high sintering temperature [4]. In order to protect the copper nanoparticles from oxidation, a number of approaches have been proposed, for example, graphitic, polymeric or legend coatings. These coating materials will hinder inter-particle contact and hence conductivity unless removed in a subsequent sintering step. Thereby, using alloy nanoparticles were desired approach to improve stability.

Copper-zinc alloy nanoparticles are more stable than pure copper [27]. Alloy nanoparticles have some properties different from those pure materials such as low density, and high strength [5, 6]. Thus, it becomes of interest because we can control the composition, crystalline phase [7] and morphology of nanoparticles to develop new nanophase materials with unique properties for many applications.

Alloy nanoparticles have been synthesized by several techniques including wet chemical, laser ablation [8], ball milling [7], and γ-ray irradiation [9]. Arc discharge technique is one of simple and efficient methods that can be used to synthesize metal nanoparticles [8-13].

Arc discharge method has been used in synthesis both of copper and alloy nanoparticles. For example, Cu_2O/CuO particles were formed by submerged arc of Cu rod in dielectric liquids, and ascorbic acid was then used for eliminate oxide. Thus, 10-15 nm Cu nanoparticles were obtained [14]. Different atmospheres (He, N_2 and Ar) were used as media of arc synthesis. The media used affected size of Cu nanoparticles [13]. Cu_5Zn_8 nanoparticles were synthesized under pure argon and had highly phase purity [15]. Moreover, uniform nano-$CuZn_5$ and nano-Cu/ZnO was synthesized from Cu/Zn rod (63/37 wt %) by arc fabrications in different medias. It

shows that the synthesis in open air related to highest amount of nano-ZnO and small CuZn nanoparticles formed in distilled water and ethylene glycol [6]. However, synthesis of metal nanoparticles by this method also incurs minor products of metal oxide. The arc discharge technique has the potential to produce nanoparticles by optimizing different parameters such as the arc discharge current, the arc chamber atmosphere, the chamber pressure etc. [15]. Moreover dielectric liquid and temperature used in discharge system are important factors for control of the chemical compositions and morphology of nanoparticles [6, 13, 15, 16]. Thus, research of appropriate conditions of its synthesis system becomes of interest.

Printing and sintering techniques are also important for printed electronic. Sintering temperature and time significantly related to electrical resistivity of the conductive patterns obtained [17, 18]. Moreover, the physical nature of printed pattern surface such as roughness and thickness inevitably affect conductivity of the conductive pattern [19].

1.2 Objective of the research

The present work have objectives to study the synthesis of copper-zinc alloy nanoparticles by arc discharge method, the effect of different dielectric liquids, the effect of storing and the effect of binder on composition and morphology of nano-structured including investigate the sintering of conductor lines on film plates.

1.3 Scope of the research

1.3.1 The arc discharge system

- The proportion of copper 90 %wt and zinc 10 %wt of wire is used as a raw material.
- The power of arc discharge system is direct current (DC) at 5 A. and 25.6 V.

1.3.2 Study the effect of dielectric liquids

- The media of arc discharge system are 4 types of dielectric liquids include deionized water, ethanol, ethylene glycol and diethanolamine.
- The nanoparticles synthesized are characterized by X-ray diffraction (XRD), transmission electron microscope (TEM), and scanning electron microscope (SEM).

1.3.3 Preparation of conductive ink

- The wires amount 20 centimeters is synthesized in dielectric liquids 150 ml.
- Silver complex solution is used as binder for conductive ink.
- The Cu-Zn ink is characterized by thermal gravimetric analysis (TGA) and differential scanning calorimetry (DSC).

1.3.4 Study the effect of sintering of printed pattern

- The inks synthesized are printed on a polyethylene terephtatate (PET) substrate.
- The pattern printed is sintered under vacuum at 80 and 100 °C for 30-120 min.
- The patterns are characterized by X-ray diffraction (XRD) and scanning electron microscope (SEM).

1.4 Expected benefits

1.4.1. Synthesis alloy metal to small particle until nano scale by using arc discharge method.

1.4.2. Appropriate conditions of conductive ink production and electrical pattern sintering.

CHAPTER II

LITERATURE REVIEW

2.1 Synthesis of metal nanoparticles by arc discharge method

Arc discharge technique has been extensively studied. Well conductive metals including silver and copper were synthesized by this technique. Follow as.

2.1.1 Silver

Chih-Hung Lo et al. (2007) studied morphology and phase composition of silver nanofluid was generated by the submerged arc nanoparticle synthesis system (SANSS) [16]. The silver electrodes were submerged in dielectric liquid and it was cooled by cooling medium. Silver was evaporated and then formed as silver nanoparticles. The particles were immediately condensed in dielectric liquid at low temperature and then weakly agglomeration of particles. The average particle size of silver synthesized is 6-25 nm and almost particle as spherical shape. The results of phase composition show that this synthesis method produced highly pure phase.

Ali Akbar Ashkarran (2010) successfully prepared colloidal silver nanoparticles. Arc discharge method was used for synthesis of nano-silver by titanium electrodes in $AgNO_3$ solution. The schematic diagram of the electrical arc discharge in liquid is shown in Fig. 2.1. Electron was released from decomposition of electrode and then reduced $AgNO_3$ to Ag nanoparticles which have average particle size is 18 nm. And found that by increasing the arc current; increase the erosion rate of electrodes and reduction of $AgNO_3$ [20].

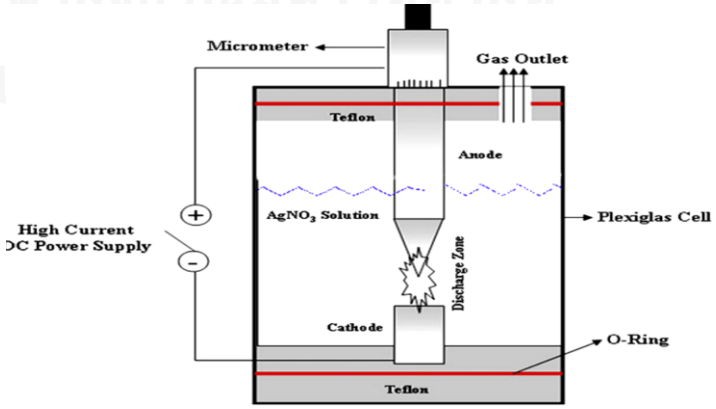

Figure 2.1 schematic diagrams showing the arc discharge process in liquid [20].

2.1.2 Copper

WEI Zhi-qiang et al. (2007) presented the synthesis of copper nanoparticles by arc discharge method. Inert gas was used as environment of arc plasma system. They suggested that can control crystallite size by controlling of discharge conditions namely increasing current and pressure of discharge system effect to increase particle size. Mean particle size about 63 nm with spherical shape of FCC structure [13].

M. Z. Kassaee et al. (2010) studied the effect of arc current on arc fabrication of copper nanoparticles. High purity rods of copper were submerged in distilled water. Current of 30-160 A were investigated. Increasing current of arc system affected particle size of copper nanoparticle to increase. At 50 A, particles synthesized easily separated by filtration and were smallest (20 nm). Copper naoparticles are brown color and minor product (CuO, Cu_2O) are black color [11].

Oxide compound of copper was formed in synthesis process of copper nanoparticles. Dielectric liquid, atmosphere and temperature of arc system are major factor of setting to copper-oxide.

2.1.3 Alloy of copper

In order to avoid forming of copper and oxygen together, new metal which more stable was developed. Alloy of copper was studied and characterized in many resources.

J.P. Lei et al. (2009) fabricated Mg-Cu alloy nanoparticles by arc discharge at 240 A and 30 V. Spherical intermetallic compounds (Mg_2Cu, $MgCu_2$, MgO) were formed by electrodes evaporation. Increasing hydrogen absorption of nanostructure of Mg_2Cu and Mg related to small particle size. The maximal hydrogen storage contents of Mg-Cu alloy nanoparticles is 2.05 wt% at 623 K [21].

A.J. Song et al. (2010) prepared 50 nm of Ni-Cu alloy particles by argon arc plasma evaporation from Ni_xCu_{1-x} ($20< x <80$ at %) bulk alloy. The highest arc temperature is 3000 °C and melting chamber was cooled by cold water. Ni-Cu alloy nanoparticles have morphology as FCC structure. The high purity and agglomeration of particle was occurred. Increasing surface energy affect to increase driving force for agglomeration and growth of nanoparticles. And also rapidly decrease of driving force related with increase of particle size [22].

2.1 Synthesis of Cu-Zn alloy nanoparticles by arc discharge method

M.Z. Kassaee et al. (2008) studied process of brass rod (Cu/Zn ratio of 63/37 wt %) is synthesized by arc fabrications. Carried out in the five different media including open air, nitrogen, distilled water, ethylene glycol, and liquid nitrogen at 100 A. Brass and zinc oxide nanoparticles is formed. The highest amount of nano-zinc oxide is formed in the open air [6]. It is shown in Fig 2.1.

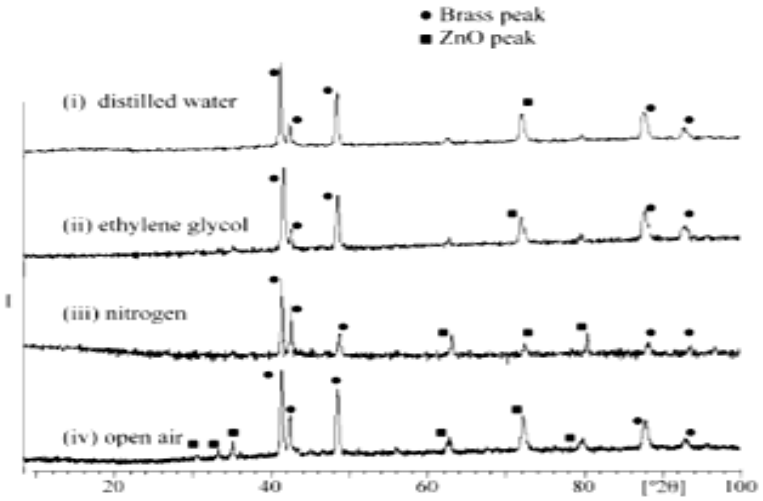

Figure 2.2 comparison of theXRDpatterns the golden nanobrass and ZnO products obtained after the arc discharge treatments in different media (i–iv): brass peak (•); ZnO peak (■) [6].

The golden nanobrass (nano-$CuZn_5$) is formed with 30-108 nm diameters. The smallest and largest nanobrass is formed in distilled water and ethylene glycol, respectively. Distilled water is chosen for the arc synthesis of nanobrass in this present.

Mansoor Farbod and Alireza Mohammadian (2014) have summarized that arc current of discharge system affected size and phase purity of Cu-Zn alloy particle [15]. Spherical particle and uniform distribution were occurred at a current of 300 A under Ar gas at a pressure of 1 atm with a average particle size of 21 nm and this results were shown in Fig. 2.2. Cu-Zn alloy nanoparicles was synthesized form bar electrode of Cu(61%)-Zn(39%). The major phase is Cu_5Zn_8, 98% of phase purity. The percentage of approximate phase was calculated by equation (1), follow as.

X phase (%) = $\frac{\sum I\,(xphase)}{A} \times 100$ X = {Cu_5Zn_8, Cu(61), Zn(39), ZnO} ----- (1)

Where, I is the intensity of different peaks.

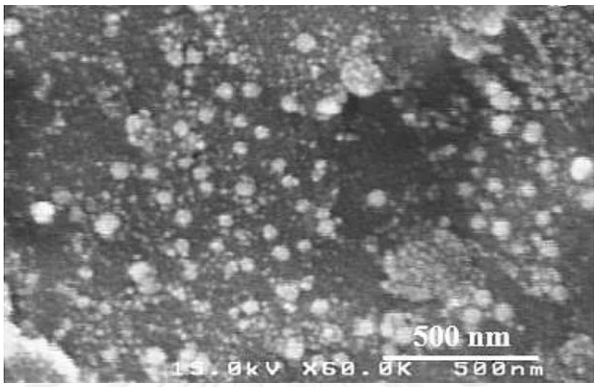

Figure 2.3 the SEM image of Cu-Zn nanoparticle synthesized at arc current of 300 A and 1 atm of Ar [15].

Cu_5Zn_8 nanoparticles were annealed at different temperature. The result shown that the disorder phase was produced at temperature range of 400- 480 ℃.

2.2 Sintering of metal conductive ink for flexible electronic

Chen et al. (2012) developed silver ink for make the conductive pattern on PET sheet [17]. Ethanolamine was decomposed as formaldehyde (equation 1) and silver oxide was added into ammonia solution (equation 2). Both solutions were mixed and then occurred as silver nanoparticles.

$$HN(CH_2CH_2OH)_2 + 2OH^- + 2H_2O \rightarrow 2HCHO + 2HCOO^- + NH_3 \quad (1)$$

$$Ag2O + 4\,NH_3 + H_2O \rightarrow 2[Ag(NH_3)_2]^+ + 2OH^- \quad (2)$$

$$HCHO + 2[Ag(NH_3)_2]^+ + 2OH^- \rightarrow HCOONH_4 + 2Ag + 3NH_3 + H_2O \quad (3)$$

Because the serial reactions in equations 1 and 2 require the existence of silver ammonia and water, the heating temperature is chosen in sections that remain both substance to avoid incomplete reaction due to solvent evaporation. Therefore, should sinter ink at temperature below boiling point of water (100 ℃).

C.K Kim et al. (2014) presented a one-step synthetic method of Cu/Ag core–shell nanoparticles with high oxidation resistance and electrical conductivity for

printed electronics on flexible substrates [23]. To obtain a homogeneous Ag coating on Cu nanoparticles, various Cu–Ag nanoparticles were synthesized with the change of [Cu]/[Ag] molar ratio using modified wire evaporation method. The Cu/Ag core–shell nanoparticles prepared at the optimum [Cu]/[Ag] molar ratio were dispersed in ethylene glycol and the nanoink was coated on a polyimide film using a screen-printing method. The Cu/Ag film sintered at 200 °C exhibited an electrical resistivity of 8.2 μΩ cm, which was much lower than the reported values for the Cu/Ag films prepared by chemical reduction or electrochemical deposition method.

B. Lee et al. (2009) have developed a copper metal-organic-based conductive ink which can be applied to printing and roll-to-roll processes [24]. The metal content is in the range of 22-26%. Regardless of annealing temperature, resistivity is saturated to a certain value after about 30 min. This means that at least 30 min of annealing time is required. The resistivity of the conductive film, after annealing under the condition of 3% H_2 is 5.4 l μΩ cm at 250 °C, 4.4 l μΩ cm at 320 °C and 4.1 l μΩ cm at 400 °C. Variations of resistivity and FE-SEM images of surface copper film after annealing at various conditions were show in Fig. 2.4. We successfully demonstrated a printable copper nano ink that proceeds to form highly conductive metal film when annealed at low temperature on flexible substrates.

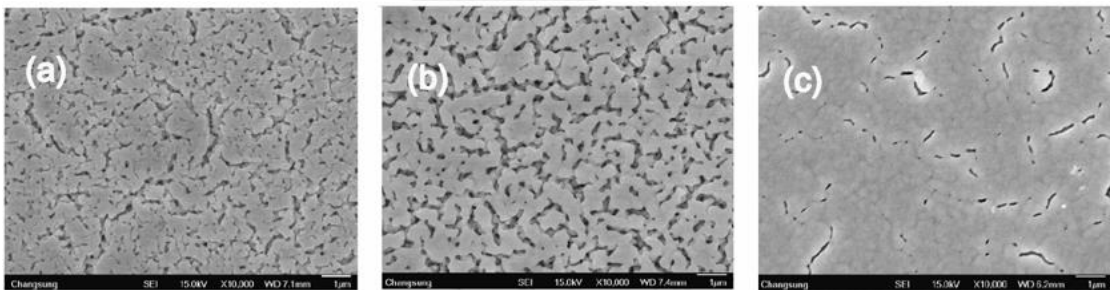

Figure 2.4 variations of resistivity and FE-SEM images of surface copper film after annealing at various conditions: (a) 250 °C, (b) 320 °C, and (c) 400 °C [24].

CHAPTER III

FUNDAAMENTALS

3.1 Conductive ink technology

Conductive inks can be a more economical way to lay down a modern conductive traces when compared to traditional industrial standards such as etching copper from copper plated substrates to form the same conductive traces on relevant substrates, as printing is a purely additive process producing little to no waste streams which then have to be recovered or treated.

Conductive inkjet technology has developed a revolutionary two-step process to create solid copper circuitry directly from digital files. The process patterns a catalytic ink and then immerses the image in an electroless plasting solution to deposit solid metal onto the desired pattern. It has developed several ink technologies to create conductive patterns using cutting edge inkjet printing technologies. R&D circuit is conducted on several different platforms utilizing common substrates such as PET, glass, silicon, and others.

3.2 Plasma nanoscience

An electric arc, or arc discharge, is an electrical breakdown of a gas that produces an ongoing plasma discharge, resulting from a current through normally nonconductive media such as air. An arc discharge is characterized by a lower voltage than a glow discharge, and relies on thermionic emission of electrons from the electrodes supporting the arc. An archaic term is voltaic arc, as used in the phrase "voltaic arc lamp".

The arc discharge is a high-current, low-voltage discharge, in contrast with the low-current, high-voltage glow discharge. It is characterized by a negative-resistance V-I characteristic, and high temperatures. Electrons for the discharge are supplied by a cathode spot that is a much more efficient electron emitter than the glow discharge cathode phenomena. The current density in the cathode spot is high and constant, so it adjusts its size to suit the discharge current. The electrons are liberated either by thermionic emission, or by high-field emission. Figure 3.1 show the schematics of the interelectrod gap. The relative importance of these mechanisms has long been in dispute, but it is convenient to assume that the fixed cathode spot of refractory electrodes (such as carbon or tungsten) is thermionic, while the

wandering cathode spot of low-melting-point cathodes (such as mercury) is high-field. A typical current density for a thermionic cathode spot is 470 A/cm^2, and of a high-field spot, 4000 A/cm^2.

An arc can be started either by a transition from a glow discharge, or by separating contacts already carrying current. If we increase the current in a glow discharge, we enter a region in which the width of the cathode fall decreases (the "abnormal glow"). This causes the ion energy to increase, and the cathode becomes heated. In arcs with thermionic cathodes, the transition is gradual as the thermionic emission increases with temperature and the discharge voltage decreases. With field-emission cathodes, such as with mercury, the transition may be sudden, as a cathode spot is created at some favorable spot. The mercury is initially in liquid form, either as a pool or as a drop, and must be raised to a temperature where the mercury vapor pressure will support the discharge. Starting a mercury arc always requires some special action, either a separately heated cathode or an ignition electrode. The pressure can also be increased to start an arc if a glow discharge already exists. The current rises as the square of the pressure, so a critical value is soon reached.

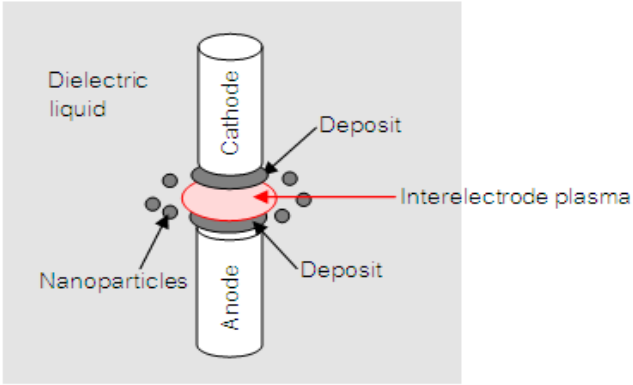

Figure 3.1 schematics of the interelectrod gap [31].

Inside the growth region, vapor flux contributing to be growth consists of neutrals and ions of metal. The nanoparticles are negatively charged due to high mobility of electrons, creating a sheath of thickness close to Debye length, and hence ions are attracted toward the nanoparticle as shown in Fig. 3.2. Nanoparticle of diameter d_{np} is surrounded by Debye sphere of radius $d_{np}/2+\lambda_{De}$ consisting of nonneutral plasma. Ions enter the sheath with Bohm speed, v_B at the Debye sphere edge, and create a focused flux that contributes to the growth of nanoparticle.

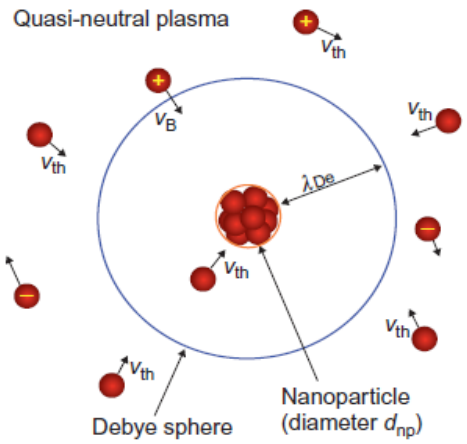

Figure 3.2 nanoparticles growth in plasma, the positive ions is focused on to the cluster from Debye sheath edge with Bohm velocity and neutrals approach the cluster with thermal velocity [31].

3.3 Brass properties

Brass is the generic term for a range of copper-zinc alloys with differing combinations of properties, including strength, machinability, ductility, wear-resistance, hardness, colour, antimicrobial, electrical and thermal conductivity, and corrosion resistance. Brasses set the standard by which the machinability of other materials is judged and are also available in a very wide variety of product forms and sizes to allow minimum machining to finished dimensions. Brass does not become brittle at low temperatures like mild steel. Brass also has excellent thermal conductivity, making it a first choice for heat exchangers (radiators). Its electrical conductivity ranges from 23 to 44% that of pure copper.

Brasses are resistant to corrosion in many media. Please consult Austral Wright Metals for detailed advice on your application. Brasses are particularly susceptible to corrosion by solutions containing ammonia or amines. Alloys with more than about 15% of zinc may suffer dezincification, which leaves a weak, porous corrosion deposit of copper. Resistance to dezincification is greatly reduced by the addition of a small amount of arsenic to the alloy. Stress corrosion cracking, particularly by ammonia and amines, is also a problem with the brasses. Alloys containing more than about 15% zinc are most susceptible. Use of the annealed temper, and annealing or stress relieving after forming, reduces susceptibility to stress corrosion cracking.

3.4 Nanometals

In nanotechnology, a particle is defined as a small object that behaves as a whole unit with respect to its transport and properties. Ultrafine particles, ornanoparticles, are between 1 and 100 nanometers in size. Nanoparticles may or may not exhibit size-related properties that differ significantly from those observed in fine particles or bulk materials. Although the size of most molecules would fit into the above outline, individual molecules are usually not referred to as nanoparticles. Metal, dielectric, and semiconductor nanoparticles have been formed, as well as hybrid structures (e.g., core–shell nanoparticles).[8] Nanoparticles made of semiconducting material may also be labeled quantum dots if they are small enough (typically sub 10 nm) that quantization of electronic energy levels occurs. Such nanoscale particles are used in biomedical applications as drug carriers or imaging agents. Nanoparticles have unique and very different properties compared with bulk material. Thermal, optical and electrical properties of particles change dramatically as the size shift from micro to nano takes place. As an example the melting point of bulk silver is 961.8 °C while nano-sized silver readily sinters below 150 °C. The optical properties of nano particles also change as a function of particle size: as an example silver nanoparticles are extraordinarily efficient at absorbing and scattering light, thus the color of silver ink depends greatly of its particle size.

- Copper nanoparticles

Copper nanoparticles are graded as highly flammable solids, therefore they must be stored away from sources of ignition. They are also known to be very toxic to aquatic life. Copper nanoparticles can be manufactured using numerous methods. The electrodeposition method is considered by many as one of the most suitable and easiest. The electrolyte used for the process is an acidified aqueous solution of copper sulfate with specific additives. The physical properties of copper nanoparticles have density is 8.94 g/cm3, molar mass is 63.55 g/mol, melting point at 1083°C and boiling point at 2567°C. Damp reunion will affect its dispersion performance and using effects, therefore, this product should be sealed in vacuum and stored in cool and dry room and it should not be exposure to air. In addition, the Copper (Cu) nanoparticles should be avoided under stress.

- Nano-alloy

Copper is found to be too soft for some applications, and hence it is often combined with other metals to form numerous alloys such as brass, which is a copper-zinc alloy**. Copper Zinc (CuZn) nanoparticles**, nanodots or nanopowder are

spherical or faceted high surface area metal particles. Nanoscale Tin Particles are typically 10-20 nanometers (nm) with specific surface area (SSA) in the 30 - 60 m 2 /g range and also available in with an average particle size of 80 nm range with a specific surface area of approximately 12 m 2 /g. Nano Tin Particles are also available in Ultra high purity and high purity and coated and dispersed forms. They are also available as a nanofluid through the AE Nanofluid production group. Nanofluids are generally defined as suspended nanoparticles in solution either using surfactant or surface charge technology. Nanofluid dispersion and coating selection technical guidance is also available. Other nanostructures include nanorods, nanowhiskers, nanohorns, nanopyramids and other nanocomposites.

Surface functionalized nanoparticles allow for the particles to be preferentially adsorbed at the surface interface using chemically bound polymers. The composition of copper-zinc alloys can vary widely depending on the application. For use as a chemical reagent, zinc typically makes up ~90% of the material. However, alloys with similar amounts of each metal are available. The physical properties of copper nanoparticles have density is 1.17 g/cm3, molar mass is 128.93 g/mol, melting point at 870°C.

3.5 Ink binder

In printing ink manufacture, any substance in an ink that allows the ink pigment to adhere to the substrate, or printed surface, and or to keep the pigment uniformly dispersed in the fluid ink vehicle. Some printing processes require specially formulated binders to enable the ink to adhere to the substrate properly. Various types of resins are used as binders. Resins are primarily binders. They bind the other ingredients of the ink together so that it forms a film and they bind the ink to the paper. They also contribute to such properties as gloss and resistance to heat, chemicals and water. Many different resins are used, and typically more than one resin is used in a given ink. Some of these are manufactured in New Zealand (see articles) but most are not. The most commonly used resins are listed below acrylics, ketones, alkyds, maleics, cellulose derivatives, formaldehydes, rubber resins and phenolics.

Silver Oxide (Ag_2O) is a highly insoluble thermally stable Silver source suitable for glass, optic and ceramic applications. Silver oxide is a photosensitive fine black powder that decomposes above 280 °C. Oxide compounds are not conductive to electricity. However, certain perovskite structured oxides are electronically conductive finding application in the cathode of solid oxide fuel

cells andoxygen generation systems. They are compounds containing at least one oxygen anion and one metallic cation. They are typically insoluble in aqueous solutions (water) and extremely stable making them useful in ceramic structures as simple as producing clay bowls to advanced electronics and in light weight structural components in aerospace and electrochemical applications such as fuel cells in which they exhibit ionic conductivity. Metal oxide compounds are basicanhydrides and can therefore react with acids and with strong reducing agents in redox reactions. Silver Oxide is generally immediately available in most volumes. High purity, submicron and nanopowder forms may be considered. Additional technical, research and safety (MSDS) information is available. It is a fine black or dark brown powder that is used to prepare other silver compounds.

3.6 Screen printing

3.6.1 Flexible substrates

Printed electronics allows the use of flexible substrates, which lowers production costs and allows fabrication of mechanically flexible circuits. While inkjet and screen printing typically imprint rigid substrates like glass and silicon, mass-printing methods nearly exclusively use flexible foil and paper.

Table 3.1 physical properties of plastic material for substrates.

Physical property	PMMA	PC	PET	Grass
Light transmittance (%)	93	89	87	93
Tensile strength (MPa)	68	65	72.5	
Grass transition point (°C)	100	150	80	
Dielectric constant at 1 MH	3	3	3	

*PMMA: Poly(methyl methacrylate) , PC: poly carbonate, PET: polyethylene terphthalate

Polyethylene terphthalate (PET) is a polyester resin obtained through the polycondensation of terephthalic acid and ethylene glycol. Its chemical structure is shown in Fig. 3.4.

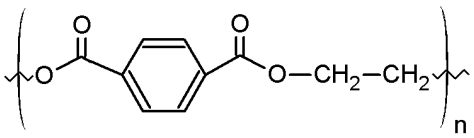

Figure 3.3 structure formula of polyethylene terphthalate.

PET is inferior to polyimide in terms of heat resistance (Tg: 80°C). However, since it is inexpensive (costing up to 320 baht per kg), PET is used in some printed circuit boards for large circuitry not requiring soldering. Furthermore, since PET is transparent and possesses relatively balanced mechanic-physical properties, it is used in a wide range of applications, including displays and solar cells. PET film on which a transparent electrode (ITO: indium tin oxide) film has been formed are being sold commercially, and are often used as device substrates. Crystalline polymer films, such as PET film, maintain their mechanic-physical properties based on biaxial stretching and thermal fixing following formation. However, since PET films have inferior thermal contraction rates compared to amorphous polymer films, and are problematic in terms of optical isotropy, they are not suitable to LCD applications. PET films are being marketed for use in relatively low-end displays such as organic EL panels and electronic paper displays.

3.6.2 Screen printing method

In the screen printing method, ink (paste) is placed on a tightly stretched screen, and then a squeegee (normally a urethane rubber blade) is pressed against and moved across the screen, thereby pushing the paste through the screen mesh and transferring the image on the screen onto the surface of the material being printed (Fig. 3.5). Like the inkjet method, screen printing is an additive method that results in little material waste, and is an especially effective process for manufacturing displays, such as PDP (plasma display panels) and organic EL panels.

Screens were previously made of silk (which is why screen printing used to be called silkscreening), but now they are typically made of a metal (mainly stainless steel), or a synthetic fiber such as polymer. The paste consists of resin and solvent in which a base material, such as a metal powder or a semiconductor, is dispersed, and must have an appropriate level of viscosity.

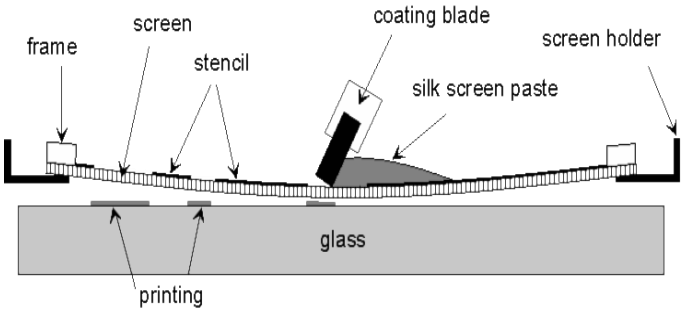

Figure 3.4 screen printing concept.

Screen printing is an off-constant printing method in that a gap (clearance) of 1 to several mm is provided between the screen and medium to be printed (substrate). The screen only contacts the substrate for an instant, while the squeegee is passing over the screen, transferring the paste. Thus, while screen printing can also be classified as a contact-type printing method, the effect of the contact on the substrate is considered less than in relief printing, for example, in which a stamp is pressed against the printing medium.

Screen printing can be divided into several methods, including 'solid printing' in which a printing film is formed over the entire surface of the printing medium, 'pattern printing' in which a printing film is formed according to a pattern, and 'plugging printing' in which via holes in a printed circuit board are plugged. Pattern printing is mainly utilized as the direct writing method for manufacturing electronic devices. In pattern printing, both areas that do not allow the paste though are formed in the screen (stencil marking) and are used for printing the pattern. To form the printing pattern, a photosensitive emulsion is applied over the entire screen and is then exposed and developed via a photomark, creating open areas.

3.7 Sintering process

3.7.1 Sintering mechanisms

Sintering is usually classified into several types based on the mechanisms that are thought to be responsible for shrinkage or densification. Sintering proceeded by solid-state diffusion falls under solid state sintering. Polycrystalline materials are usually sintered by this process. On the other hand, amorphous materials are sintered by viscous flow and are considered to undergo viscous sintering. Another type of sintering that makes use of a transient second phase that exists as a liquid at the sintering temperature is known as liquid phase sintering. The liquid phase under the right conditions can provide a path for rapid transport and, therefore, rapid

sintering. Finally, processes that make use of an externally applied pressure to enhance densification are classified under pressure assisted sintering.

The entire sintering process is generally considered to occur in three stages: initial stage, intermediate stage, and final stage. There is no clear-cut distinction between the stages since the processes associated with each stage tend to overlap each other. However, some generalizations can be made to distinguish one stage from the next. In the initial stage, particles can be rearranged into more stable positions by rotating and sliding in response to the sintering forces. This contributes to shrinkage and an overall increase in density. During particle rearrangement, there is an increase in interparticle contact, enabling the formation of necks between particles. Neck formation and growth can take place by diffusion, vapor transport, plastic flow, or viscous flow.

Polycrystalline materials generally are sintered by diffusional processes while amorphous materials densify by viscous flow. The driving force for all the mechanisms is the tendency of the material to reduce its chemical potential or energy. This is accomplished by material transport from regions of high energy to regions of lower energy. Surfaces, interfaces and grain boundaries have associated energies that depend on surface or boundary curvature. By eliminating or minimizing these surfaces or by reducing their curvature, the overall energy of the material is reduced. The driving force for sintering is a decrease in the surface free energy of powdered compacts, by replacing solid-vapour interfaces. Thermodynamically, then, sintering is an irreversible process in which a free energy decrease is brought about by a decrease in surface area. The development of microstructure and densification during sintering is a direct consequence of mass transport through several possible paths (one of these paths is usually predominant at any given stage of sintering):

- Gas phase (evaporation/condensation)
- Liquid phase (solution/precipitation)
- Solid phase (lattice diffusion)
- Interfaces (surface diffusion, grain boundary diffusion)
- Viscous or plastic flow, under capillary pressure (internal) or externally appliedpressure (pressure-sintering, hot-pressing, hot-isostatic-pressing)

3.7.2 Nanomaterial Sintering

Nanomaterial refers to the material with the feature size from 1 to 100 nm. Compared with conventional microscale materials, nanoscale material has significantly larger surface energy. Thus, reducing the silver particle size from the microscale to the nanoscale range can theoretically lower the sintering temperature.

However, because of sintering is a processing which depends on atomic diffusions, the densification rate is not only determined by how easy the atoms can diffuse, but also by how they diffuse.

The first challenge associated with nanoscale material sintering is the agglomeration/aggregation of the nanomaterials. Agglomeration and aggregation are more likely occur in nanomaterials due to their fine particle sizes. Agglomeration is a procedure that the pre-sintering powder compacts are attracted together by weak forces such as Van der Waals/electrostatic forces; while aggregation is a procedure that the pre-sintering material is bonded together by solid necks of significant strength such as metallic force. One of the major differences between agglomerate and aggregate is that the agglomerate can usually be re-dispersed by external energy such as mechanical or ultrasonic forces while the aggregate cannot. Figure 3.5 illustrates the difference between agglomeration and aggregation.

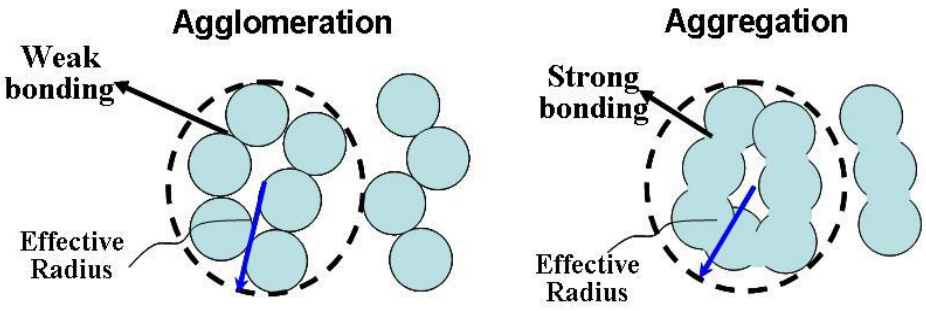

Figure 3.5 illustration of agglomeration (a) and aggregation (b) and their effective particle sizes.

Both agglomeration and aggregation result in inhomogeneous distribution of particles and thus the initial (green) density of powder compacts before sintering could be significantly lower due to the loose pack of the agglomerate/aggregate. The lower initial (green) density is detrimental for sinterability. The effective radius instead of the real radius of particle, are usually used to characterize the degenerated sintering capability of agglomerated/aggregated particles. Figure 3.5 shows that the effective radius can be much larger than that of particles. When the effective radius reaches the micron size, the advantages of nanoscale particles are lost. As discussed before, agglomerate can be re-dispersed before sintering but the aggregate cannot. Thus, aggregate should be avoided as much as possible during the preparation of nanomaterials.

Another challenge for nanomaterial sintering is the non-densifying diffusions at low-temperatures. As discussed before, for a polycrystalline material, there are least six different diffusions happen during a sintering procedure. Among the six sintering mechanisms, only volume diffusion of matter from the grain boundaries or from dislocations in the neck region can produce densification. Other diffusion of matter from surfaces cause particle necking and coarsening rather than densify them as illustrated in Fig. 3.6.

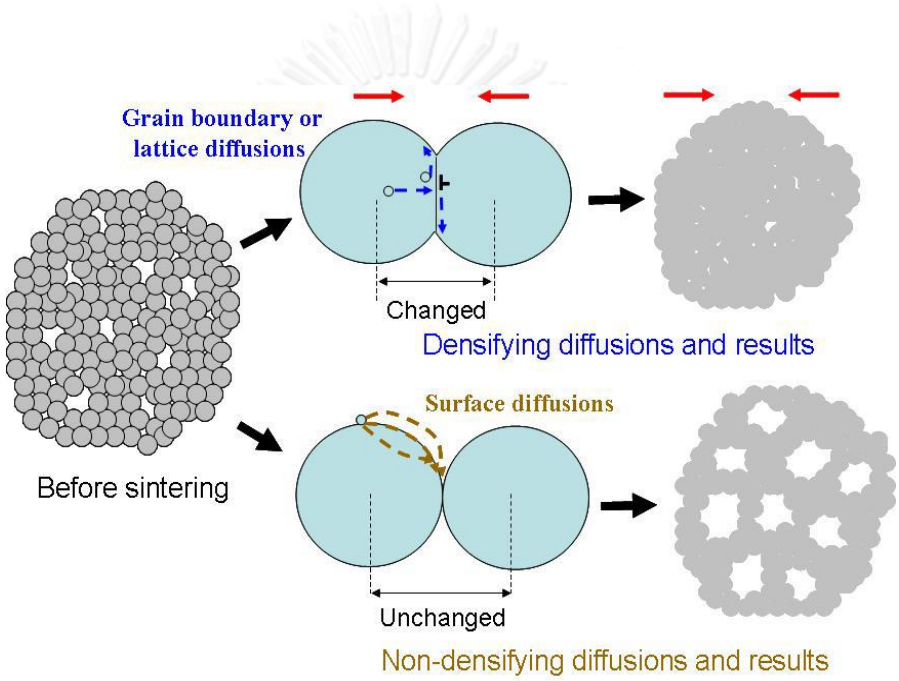

Figure 3.6 illustration of densifying and non-densifying diffusions and their sintering results.

CHAPTER IV

EXPERIMENTAL

4.1 Materials

- Brass wire (Cu /Zn; 90/10%wt)
- Ethylene glycol (QRëC)
- Ethanol (VWR)
- Deionization water
- Diethanolamine (QRëC)
- Methanol (QRëC)
- Ice and dry ice
- Silver oxide
- Ammonium hydroxide
- DC power supply (DC Inverter Arc welder, Iweld)
- Arc machines
- Coated polyethylene terephtatate (PET) film (Novacentrix)
- Screen frame
- 2% Hydrogen-nitrogen mixed gas

4.2 Study of process of the nano Cu-Zn conductive ink

4.2.1 Synthesis of Cu-Zn nanoparticles by arc discharge method

Cu-Zn nanoparticles are prepared by submerged arc discharge of copper-zinc wire (Cu/Zn: 90/10 wt. %) with diameters of 1 mm with a direct current. Arc discharge tools are set as a static cathode and movable anode, submerged in dielectric liquid. Dielectric liquid was used for cooling arc column. The schematic diagram of the Arc discharge system is shown in Fig. 4.1.

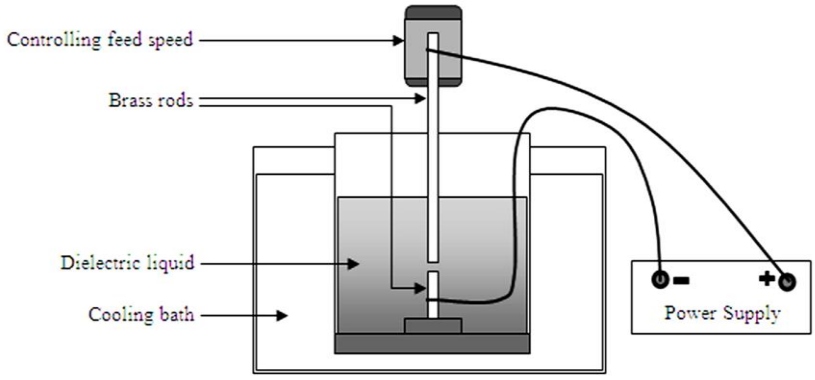

Figure 4.1the schematic diagram of the Arc discharge system.

4.2.2 Effect of dielectric liquid and storage

Four different dielectric liquids including deionized water (DI water), ethanol, ethylene glycol (EG), and diethanolamine (DEA) are used as media in discharge system. The temperature of dielectric liquids is kept constant by using cooling media. Table 4.1 show the conditions of this experiment.

The large particle is removed out of colloid solution after synthesis. It is filtrated by filter paper with size of orifice is 1 μm. Before analyzed, the particles are separated by centrifugal mechine at 10,000 rpm for 30 min, washed by methanol and then are dried at 75 °C for 30 min.

Table 4.1 the process parameter to investigate effect of dielectric liquid.

Sample	1	2	3	4
Dielectric liquid type	DI water	Ethanol	Ethylene glycol	DEA
Amounts of brass loading (g/L)	5.4	5.4	5.4	5.4
Cooling media type	Ice/water (4 °C)	Dry ice/ Ethylene glycol (-14 °C)	Dry ice/ Ethylene glycol (-14 °C)	Coldwater (15 C)

Cu-Zn nanoparticles colloid was synthesized in diethanolamine and then was stored in glass bottle for 2 month and 6 month.

4.3 Preparation of binder

Silver complex solution is selected as binder of Cu-Zn conductive ink in this experiment. Preparation of silver solution follows experimental design of Chen et al. (2012). Silver oxide is added in DI water and 33% ammonium hydroxide solution. The solution is filtered by filter paper for remove giant particle.

4.4 Preparation of Cu-Zn conductive ink

Select appropriate dielectric liquid for preparing of conductive ink after study the effect of different type dielectric liquid. 20 cm of copper-zinc rod length is utilized in submerged arc discharge system in dielectric liquid of 150 ml for 1 batch. Cu-Zn colloid solution was prepared from 3 batch of the synthesis. The nanoparticles colloid finally obtained were separated by centrifuge with 10,000 rmp for 30 min and only remained is 5 ml. Silver complex solution was prepared and mixed into colloid solution. The mixed solution was hest at 80 °C for 5 min. Summary of Cu-Zn conductive ink preparation is concluded in Fig. 4.2.

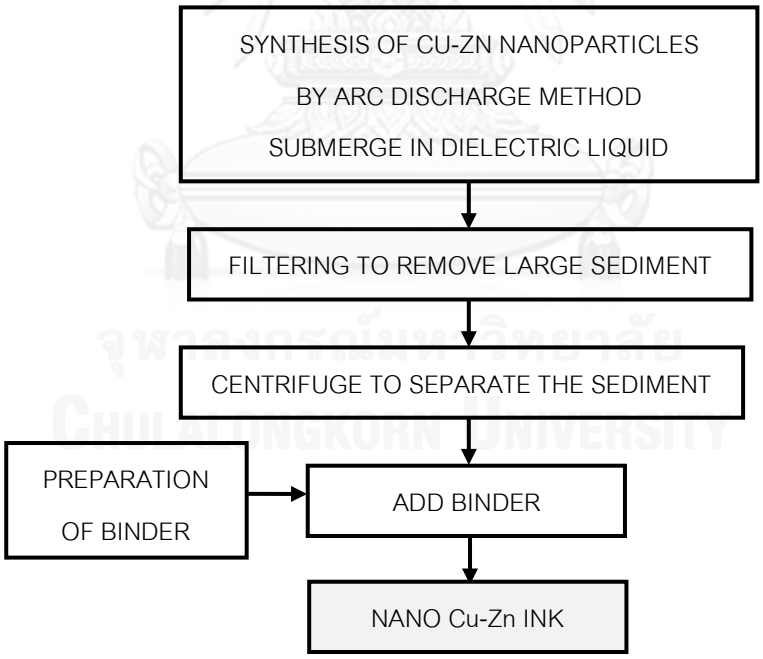

Figure 4.2 procedure of Cu-Zn conductive ink preparation.

4.5 Study of conductive pattern

4.5.1 Screen printing

Cu-Zn conductive inks are printed on a polyethylene terephtatate (PET) substrate as a two point probe pattern by screen printing. The two point probe pattern is shown in Fig. 4.3.

Figure 4.3 two point probe pattern.

4.5.2 Effect of sintering

Two ambient were used in sintering of printed film including air and 2% hydrogen-nitrogen mixed gas. Sintering in 2% H_2-N_2 mixed gas was in two steps. First, the pattern is carried out oxidize sintering at 100°C under atmosphere for 30 min. Next, them is heat at 150°C under 2% H_2-N_2 mixed gas. Both sintering were annealed for 15-60 min as show in table 4.2. Finally, the pattern is measured electric resistivity.

Table 4.2 the experimental design of sintering under different gas

Sample	Atmosphere	Time (min)
1	Air	-
2	Air	15
3	Air	30
4	Air	45
5	Air	60
6	Air $\rightarrow$ 2% H_2-N_2	15
7	Air $\rightarrow$ 2% H_2-N_2	30
8	Air $\rightarrow$ 2% H_2-N_2	45
9	Air $\rightarrow$ 2% H_2-N_2	60

4.6 Characterizations

The particles synthesized were characterized by X-ray diffraction (XRD), transmission electron microscopy (TEM) and scanning electron microscopy (SEM). X-ray diffractometer (CuK radiation) operated from 20° to 80° in the 2θ range and then identify crystalline and chemical composition. Crystallite size was calculated by Bragg's law and Scherrer equation. TEM and SEM show the morphological structure. TEM/EDS operated on JEOL JEM-2100 at 200 kV with a nickel grid and SEM/EDS operated on JEOL JSM-5800LV.

The surface of patterns printed is observed by scanning electron microscopy (SEM), Chemical composition was identified by X-ray diffraction (XRD) and Electric resistivity of circuit pattern printed was measured by LCR meter.

Thermodynamic indicator of conductive ink is analyzed by thermal gravimetric analysis (TGA) and differential scanning calorimetry (DSC).

CHAPTER V

RESULTS AND DISCUSSIONS

5.1 Synthesis, characterization and stability of Cu-Zn nanoparticles by arc discharge method in different dielectric liquid

In arc zone, Cu-Zn electrodes were blasted as plasma cloud and gas bubbles were generated. The Cu–Zn vapor were incurred in arc zone and then was condensed at low temperature in dielectric liquid for generate clusters of nanoparticles.

The morphological of the copper-zinc alloy nanoparticles synthesized were studied by the SEM and TEM images as shown in Fig. 5.1 and 5.2, respectively. The shapes of nanoparticles synthesized in four different dielectric liquids were spherical particles with nanometer size. Figure 5.1(b-d) shows a uniformly distribution of nanoparticles synthesized in ethanol ethylene glycol and diethanolamine. In contrast, nanoparticles synthesized in deionized water show a variety particles size (Fig. 5.1a). The SEM/EDX of Cu-Zn nanoparticles synthesized in deionized water and ethanol are 88/12 %wt and 90/10 %wt, respectively. The result of nanoparticles which was synthesized in ethylene glycol and diethanolamine solvent are similar, about 93 %wt of Cu and 7 %wt of Zn. The TEM images in Fig. 5.2 show spherical particles. In comparison, as reported by the morphology of Cu-Zn nanoparticles synthesized by laser ablation and melting-milling techniques were angular crystallite particles resulted from highly non-equilibrium synthesis conditions [7, 25]. The maximum size of 40-60 nm nanoparticles was obtained by synthesis in deionized water. In comparison, other dielectric liquids obtained similar average particles size of 5-20 nm. One reason is because delonized water used higher temperature (4 °C) but ethanol and ethylene glycol use only -14 °C. Higher temperature used in synthesis leads to larger nanoparticles obtained. The size of the nanoparticles synthesized depends on the growth of the critical nucleus of nanoparticles formation and the growth process of the nuclei controlled by diffusion of the growth species from bulk to the growth surface [26].Therefore, to obtain small particles, dielectric liquids with high viscosity at low temperature should be employed. The particle size is also affected by the dispersion stability that can be checked by a visual inspection of sedimentation [10].

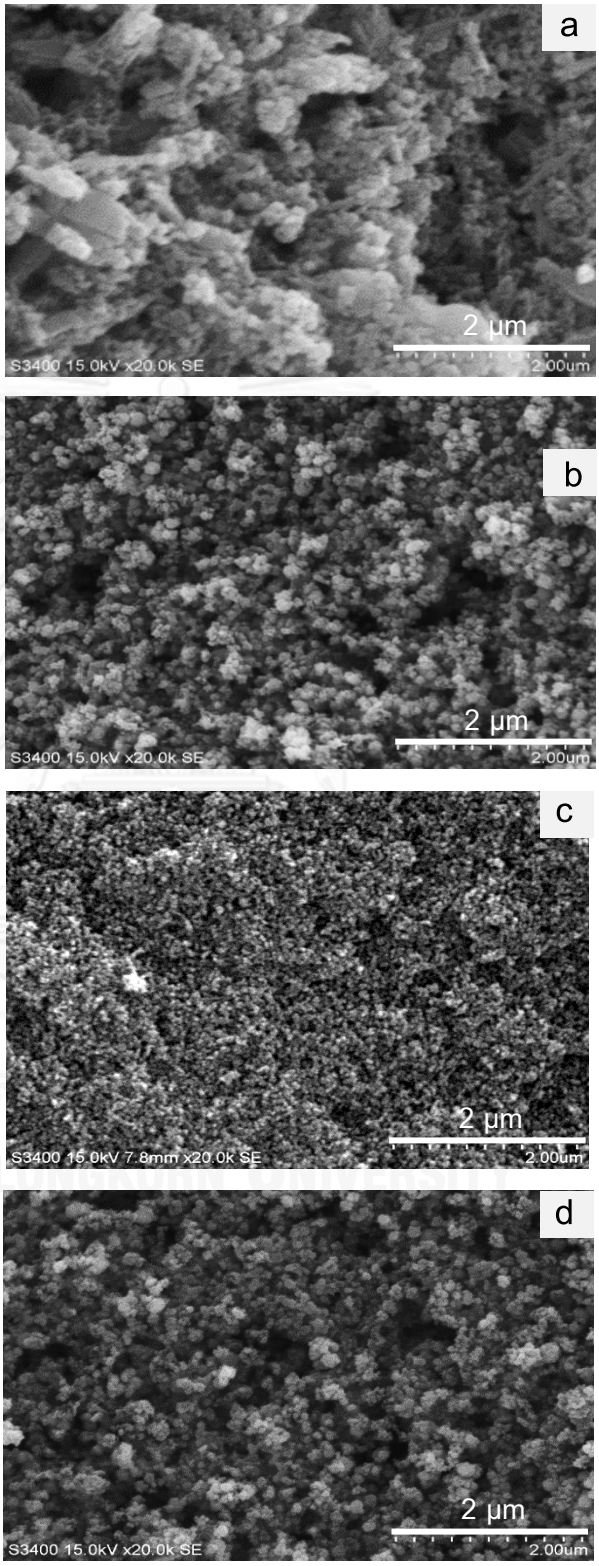

Figure 5.1 SEM images of nanoparticles synthesized in deionized water (a), ethanol (b), ethylene glycol (c) and diethanolamine (d).

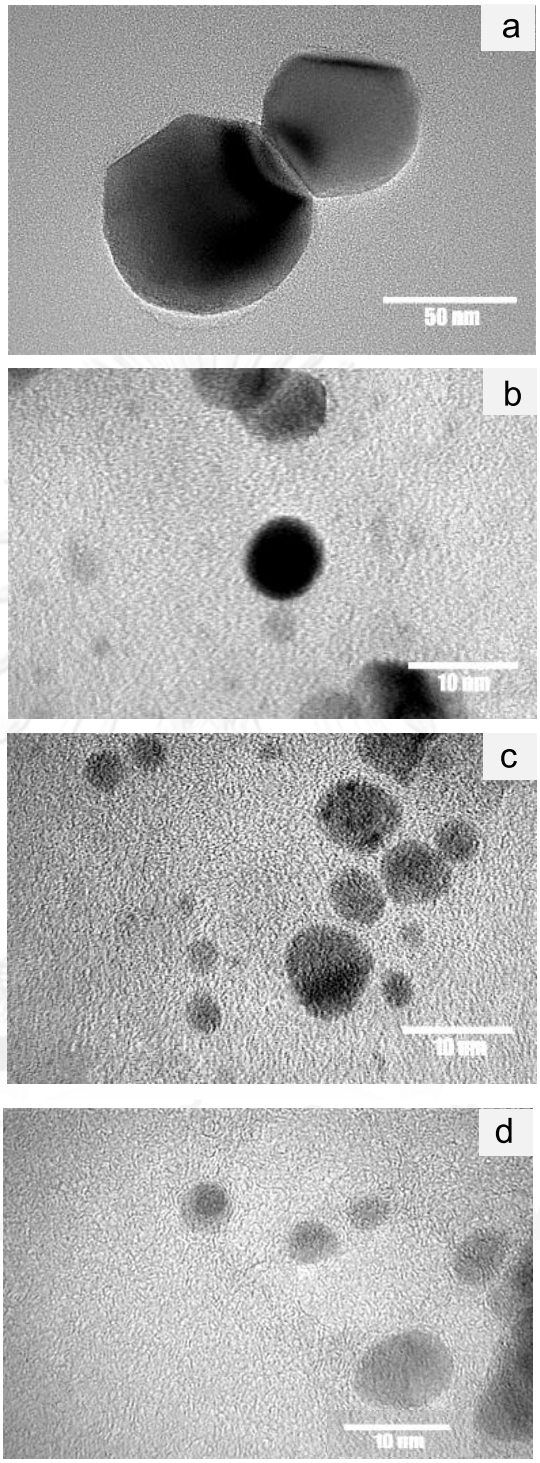

Figure 5.2 TEM images of nanoparticles synthesized in deionized water (a), ethanol (b), ethylene glycol (c) and diethanolamine (d).

Hydrogen and oxygen atoms are occurred in the arc plasma area and then form gas bubble. In addition, the oxygen free radical atoms react with Cu and Zn then produce CuO or Cu_2O and ZnO, respectively [27, 28]. Alternative, the XRD patterns of nanoparticles synthesized in all dielectric liquids do not show peak of copper-oxide (Fig. 5.3 a-d). However, the XRD results in Fig. 5.3 (a-c) of three dielectric liquids (deionized wate, ethanol and ethylene glycol) show peak of ZnO as (100), (002), (101), (110), (103) and (112). Reason that it do not produce CuO because ZnO is easier to be formed compared to CuO by the standard electrode potential of copper (E^0 = 0.34 V) is higher than that of zinc (E^0 = -0.76 V) (Chung et al, 2004 and Park et al, 2005). The XRD result of diethanolamine not show peak of metal-oxide because diethanolamine can act as a weak reducing agent and also as a capping agent in order to protect the surface of the nanoparticles, follow by equation 1 and 2 [17, 29]

$$HN(CH_2CH_2OH)_2 + 2OH^- + 2H_2O \rightarrow 2HCHO + 2HCOO^- + NH_3 \quad (1)$$

$$Cu_2O + 2HCOO^- + 2H_2O \rightarrow 2Cu + 3H_2O + 2CO_2 \quad (2)$$

The XRD pattern of the nanoparticles synthesized in four dielectric liquid show peak of Cu-Zn (111), (200), (220) which had different particle size. The average particle size of Cu-Zn in deionized water, ethanol, ethylene glycol and diethanolamine were estimated by Scherrer's equation as 61.6 nm, 26.3 nm, 11.6 nm and 25 nm, respectively. Size of the nanoparticles synthesized were estimate by Scherrer's equation, agree with the particles sizes was visual observed by TEM.

In addition, figure 5.4 show XRD pattern of Cu-Zn nanoparticles after storing in diethanolamine for 1 day, 2 month and 6 month. Three periods shows the peak of Cu-Zn and Ag. In 1 day of storing is estimate particle size as 25 nm. Increasing storing time of Cu-Zn colloid found that particle size to increase. After is stored for 2 month and 6 month, the particle size were 30 nm and 95 nm, respectively. That is because more particles together. Although, increasing time of storing affect to increase particles size. But colloid had high anti-oxidation stability (do not form metal-oxide), because have high reducing ability [30] of diethanolamine. Therefore, diethnolamine solvent is appropriate dielectric liquid in synthesis by arc method.

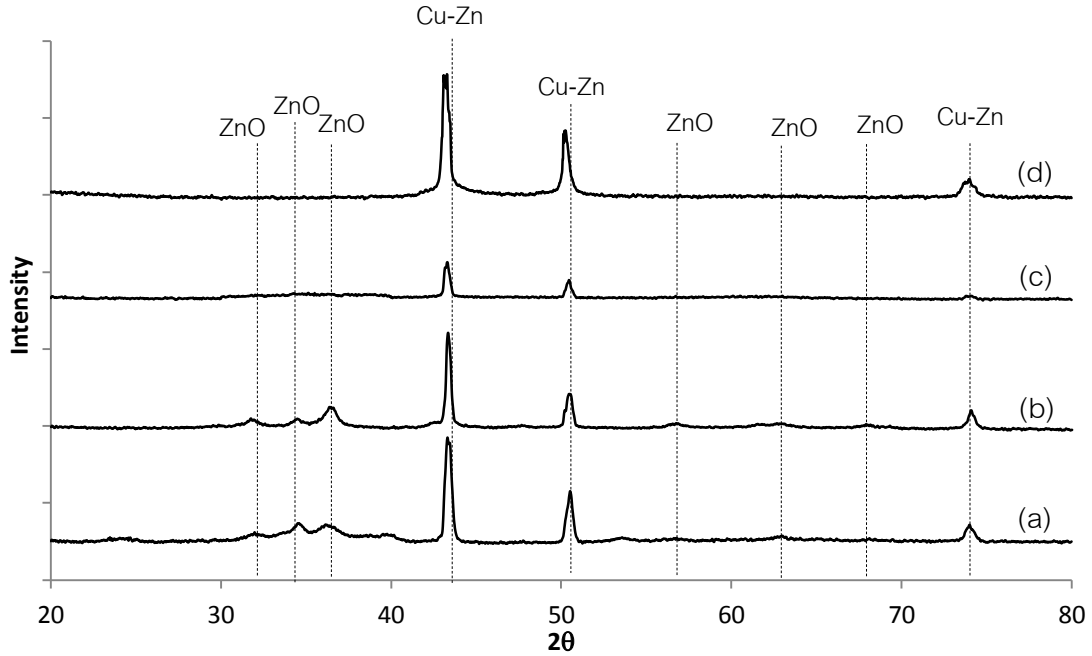

Figure 5.3 X-ray diffraction patterns of nanoparticles synthesized in deionized water (a), ethanol (b), ethylene glycol (c) and diethanolamine (d).

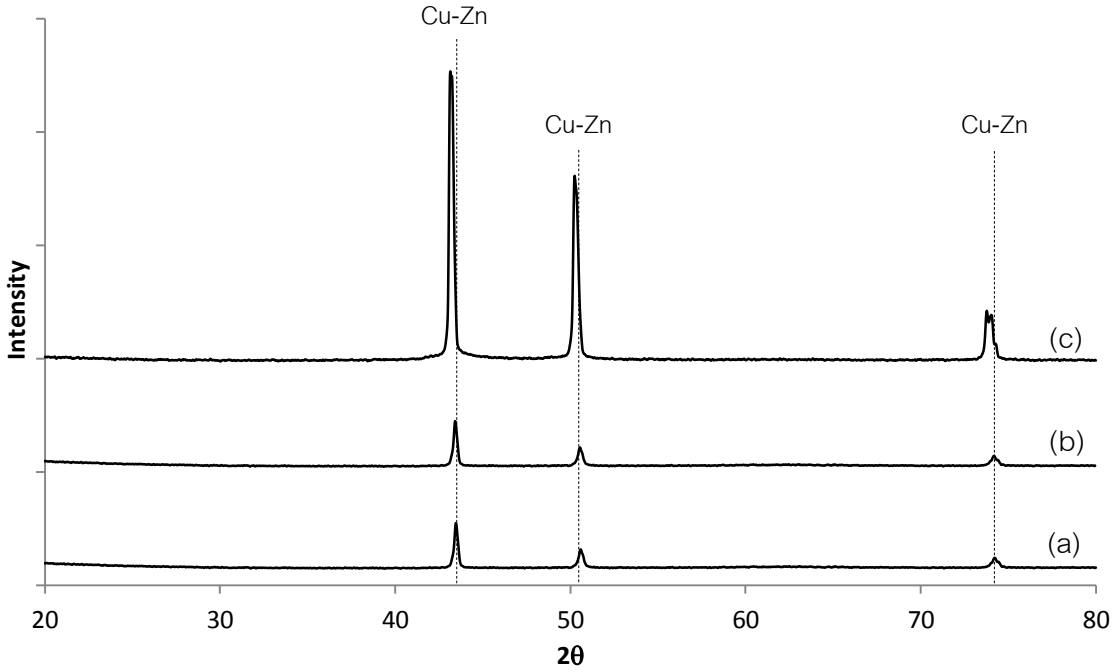

Figure 5.4 X-ray diffraction patterns of Cu-Zn nanoparticles after storing in diethanolamine for 1 day (a), 2 month (b) and 6 month (c).

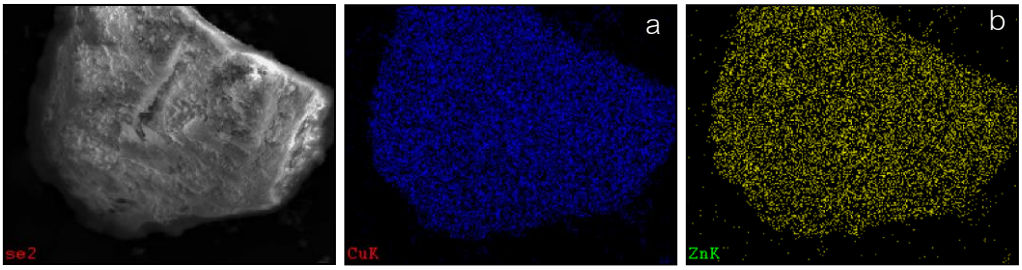

Figure 5.5 SEM/EDX images of nanoparticles synthesized in diethanolamine; (a) copper and zinc (b).

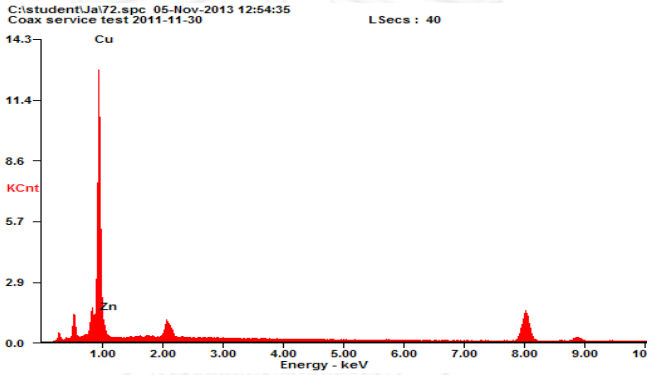

Figure 5.6 SEM/EDX patterns of Cu-Zn nanoparticles synthesized in diethanolamine.

The SEM/EDX images show nanoparticles synthesized in diethanolamine (Fig.5.5) and it shows that in one particle have mix of copper (Fig 5.5 (a)) and zinc (Fig 5.5 (b)) together. Therefore particles synthesized will form as Cu-Zn alloy and have well adhesion. Figure 5.6 show amounts of copper and zinc which synthesized in diethanolamine, copper has more than zinc and similar with ratio of Cu-Zn wire, have 88.35 wt % of copper and 11.65 wt % of zinc.

5.2 Thermal properties of the nano Cu-Zn ink

The Cu-Zn colloid solution was produce by Cu-Zn nanoparticles synthesized in diethanolamine solvent. The results of thermal gravimetric analysis for the nano Cu-Zn colloid solution were shown in Fig. 5.5. The mass loss was occurred two stages. The first stage was observed between 88 ℃ to 180 ℃ and it loses to 25% was caused by volatilization of hydrogen and oxygen. 33% of mass loss belong second stage, was found from 180 ℃ to 250 ℃ and it matches with a major of derivative weight peak, which was found at 225 ℃. This stage was evaporation of diethanolamine.

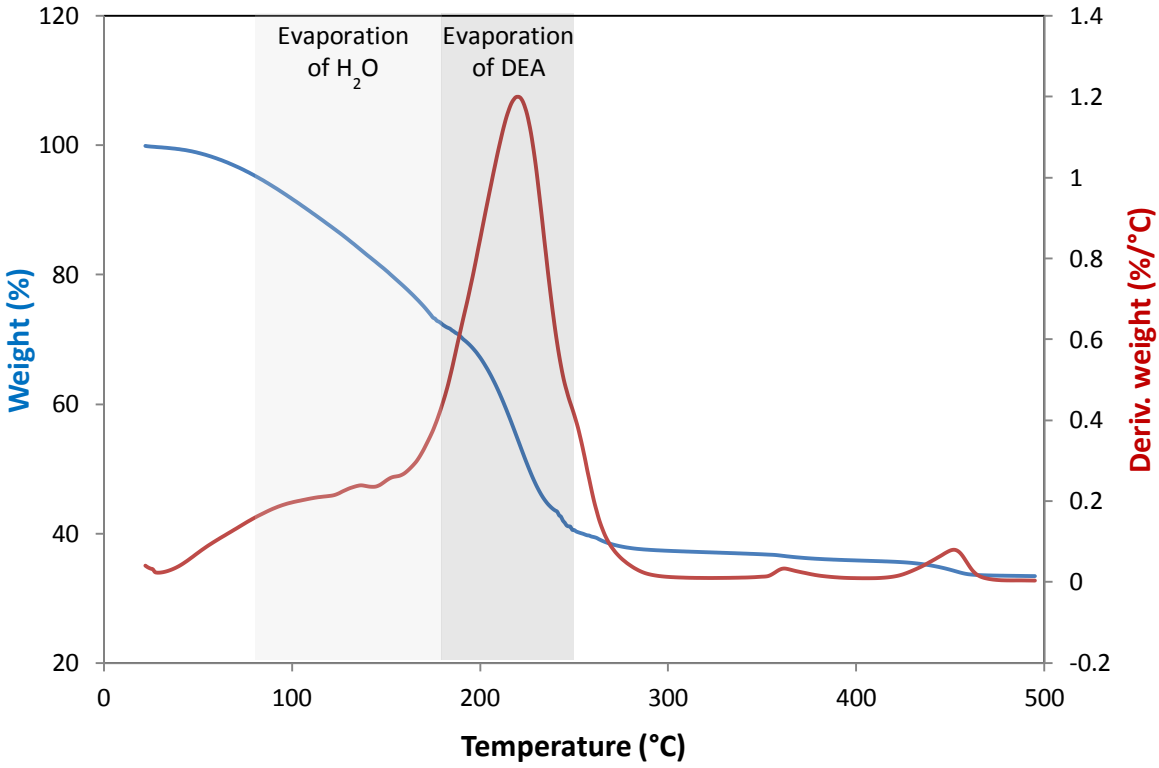

Figure 5.7 TGA/DTA curve of the nano Cu-Zn ink in air atmosphere.

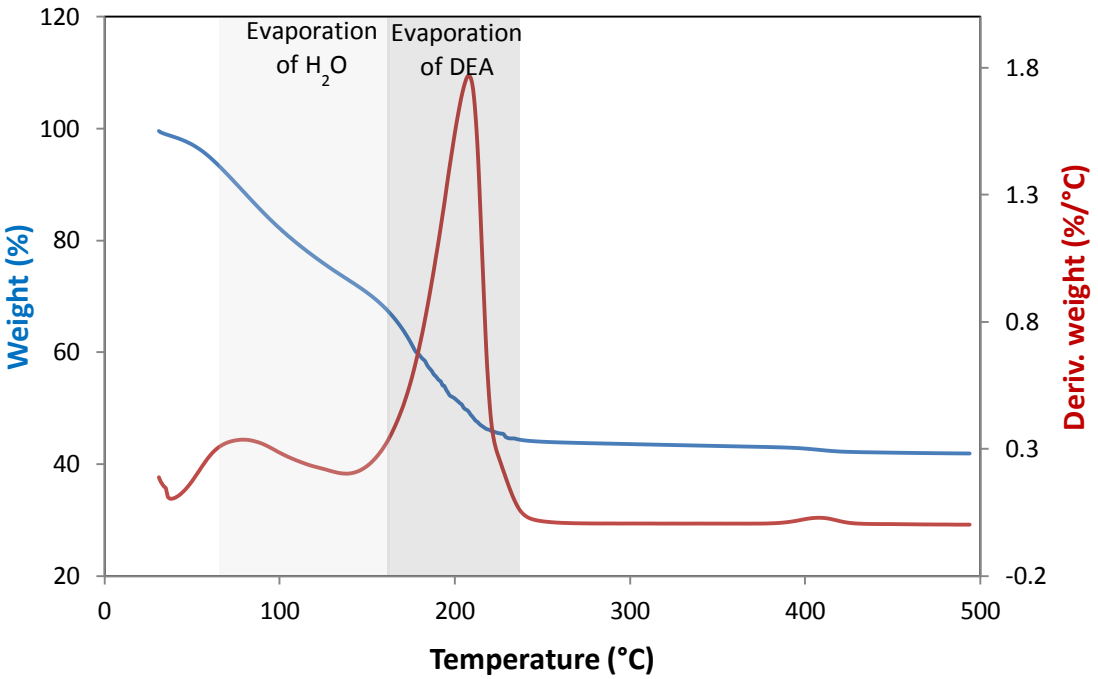

Figure 5.8 TGA-DTA curve of the nano Cu-Zn ink after silver complex binder adding.

Figure 5.7 show the results of thermal gravimetric analysis for the nano Cu-Zn ink. The final weight of ink is about 40%, which is amount of metal content. The mass loss was observed between 63 ℃ to 165 ℃. It loses to 28% because hydrogen, oxygen and ammonia were volatilized. At temperature between 165 ℃ to 225 ℃, 22% of mass loss was caused by evaporation of diethanolamine. Amount of mass loss of diethanolamine decreased to 11%. Because that it was decomposed are some formaldehyde and ammonia [17]. The result shows that increasing of time and temperature of thermal analysis, it not show the mass gain. It is possible that oxygen in air ambient can not to adhere on the surface of particle of ink.

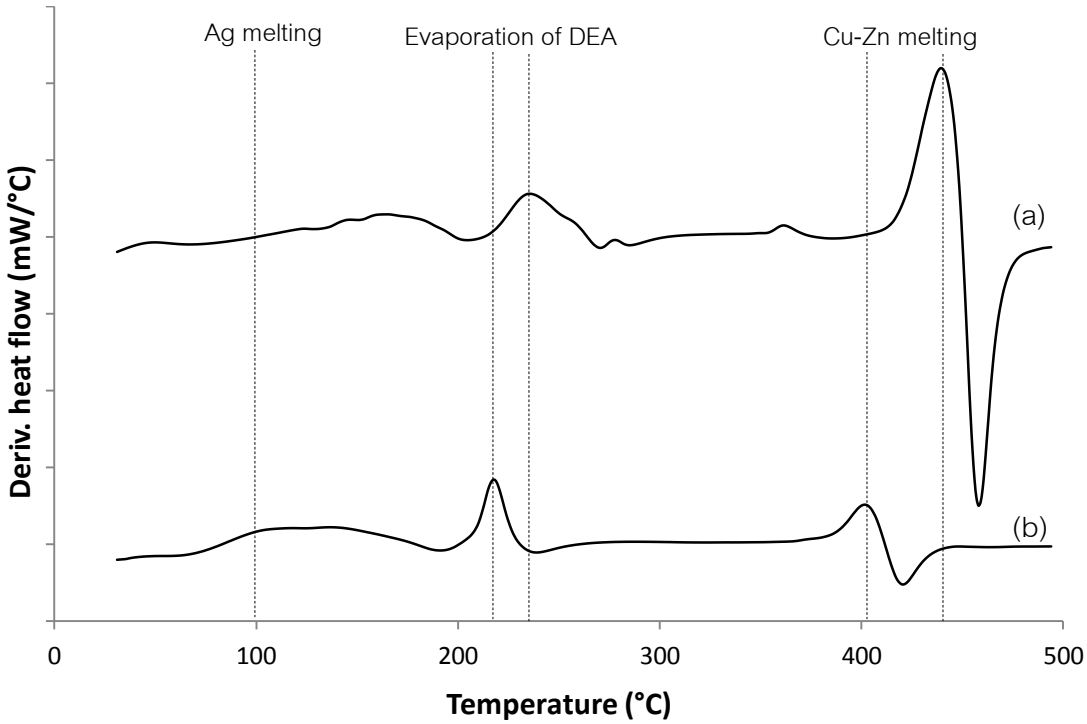

Figure 5.9 Derivative of heat flow curve of the nano Cu-Zn ink before (a) and after (b) silver complex binder adding.

The curve in Fig. 5.8 show the peak of derivative heat flow of the Cu-Zn ink before and after the ink was added silver complex binder. It shows that temperature of curing in air of Cu-Zn which binder was added will shift to left side or to decrease about 50 °C. Therefore, binder adding will decrease temperature of thermal changing. In addition, the curve show a major of derivative heat flow peak at 450 °C of Cu-Zn colloid and 400 °C of Cu-Zn ink. And that temperature should be melting temperature of Cu-Zn nanoparticles.

5.3 Sintering and conductivity of the Cu-Zn pattern

Cu-Zn conductive ink was printed on PET film and then was sintered in different ambient for 15, 30, 45 and 60 min.

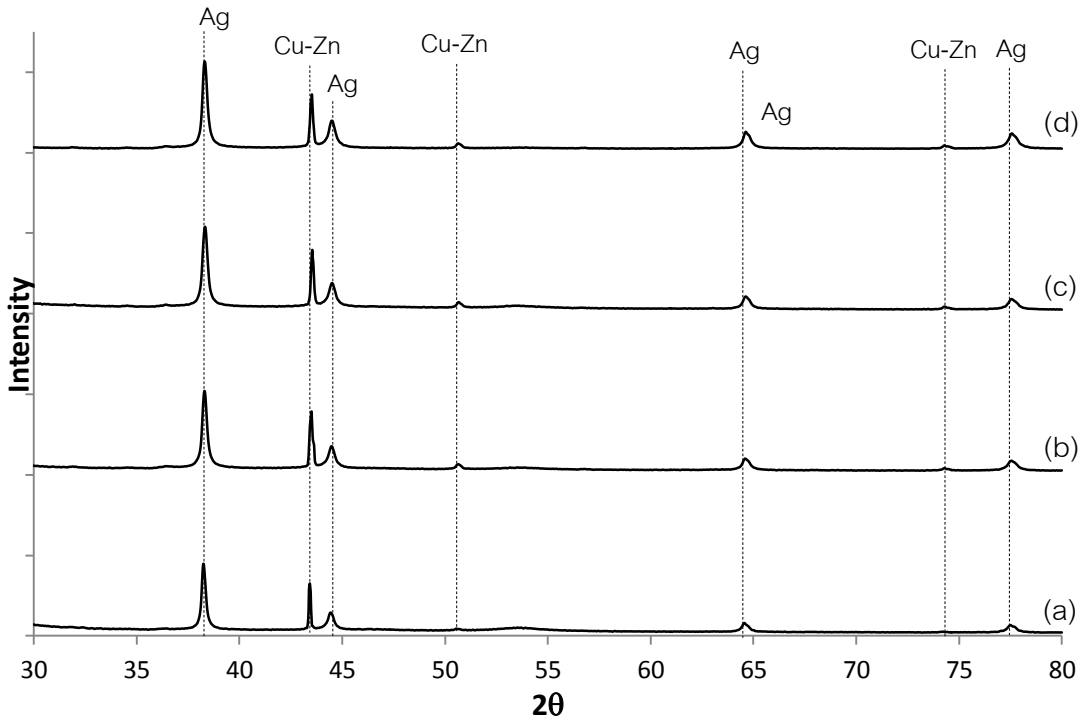

Figure 5.10 X-ray diffraction pattern of the printed film using nano Cu-Zn ink and then were sintered in air at 150 °C for 15 min (a), 30 min (b), 45 min (c) and 60 min (d).

X-ray diffraction curve of the printed films which were sintered in air at 150 °C, were shown in Fig 5.8. There XRD pattern shows the peak of Cu-Zn (111), (200), (220) and Ag (111), (200), (220), (311). Increasing the sintering time, not affect change the pattern. Scherrer's equation cannot estimate particle size because it larger than 100 nm.

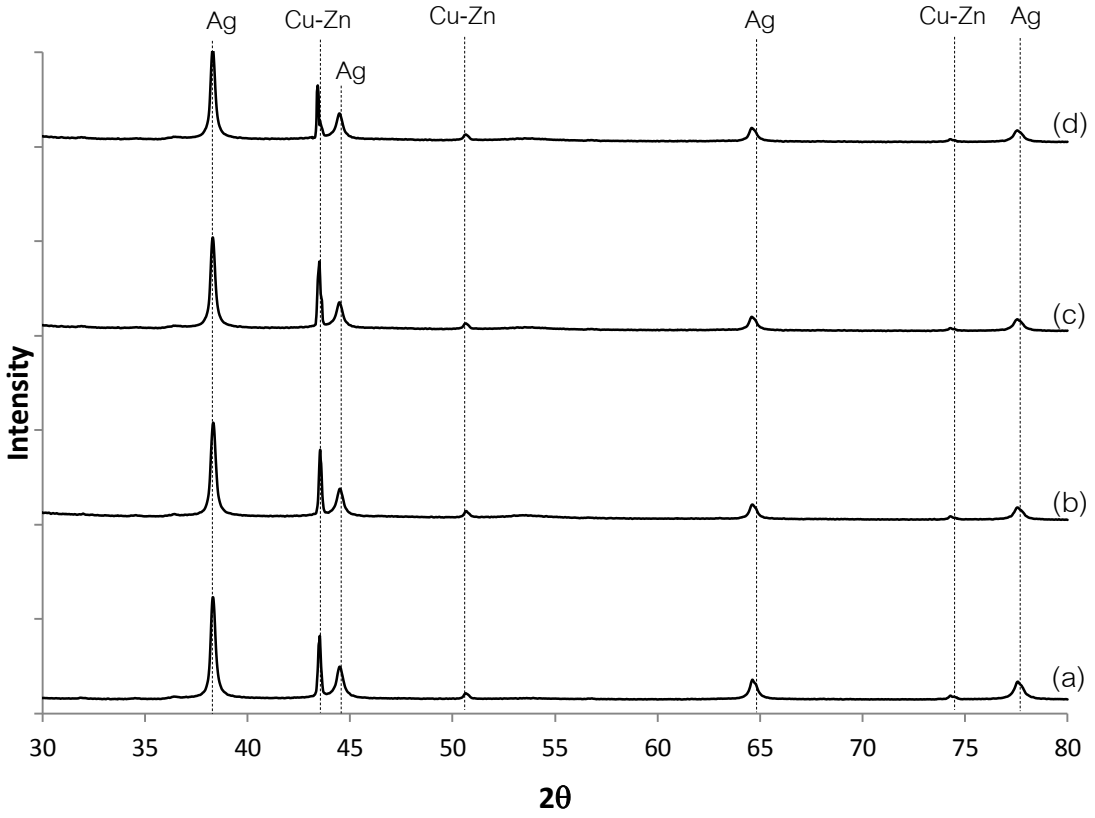

Figure 5.11 X-ray diffraction pattern of the printed film using nano Cu-Zn ink and then were heated in air at 100 ℃ for 30 min before sintering under 2% H_2-N_2 gas at 150 ℃ for 15 min (a), 30 min (b), 45 min (c) and 60 min (d).

The result of XRD pattern of the printed film using the Cu-Zn ink and then were heated in air at 100 ℃ for 30 min before sintering under 2% H_2-N_2 gas by various annealing time was shown in Fig. 5.9. Both ambient were yielded similar. That is show the peak of Cu-Zn and Ag is (111), (200), (220) and (111), (200), (220), (311), respectively.

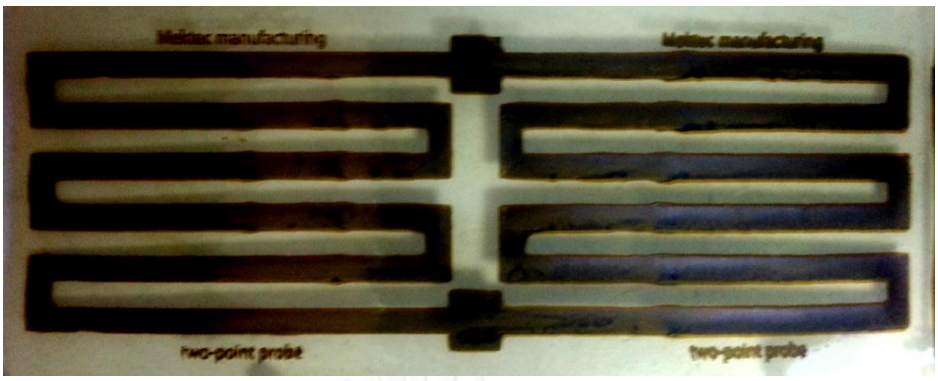

Figure 5.12 the screen printed pattern using nano Cu-Zn ink was coated on PET film after sintering at 150 ℃ in air atmosphere for 60 min.

Conductive ink was prepared from the nanoparticles synthesized in diethanolamine. It was then screen printed on PET substrate. Sintering of the patterns printed influences to morphology transition on their surface. The pattern after sintering for 60 min was show in Fig 5.10, its color is dark brown.

The morphological of Cu-Zn printed film as shown in Fig. 5.12 and 5.13. Figure 5.12 show SEM images of the printed film using nano Cu-Zn ink and then were sintered in air at 150 ℃ by using different time. At 15 min show the thickly cluster of particle (Fig 5.12 a) and the SEM/EDX of pattern contain Cu 82 %wt, Zn 8 %wt and Ag 10 %wt. Increasing sintering temperature affect the nanoparticles bind together and expanded (Fig 5.12 b and c). Cross-section of the printed pattern was sintered for 45 min not show uniform of particle because the silver binder was completely sintered. The surface of pattern after sintering for 60 min found that as sheet which was massively packed (Fig. 5.12 d). The EDX of pattern contain Cu 82.5 %wt, Zn 9 %wt and Ag 8.5 %wt for 60 min of sintering. Figure 5.13 (a) show SEM images of the printed film after sintering under 2% H_2-N_2 mixed gas at 150 ℃ for 15 min, agglomeration of nanoparticles is noticed. From result of SEM/EDX, amounts of Cu, Zn and Ag are 85.3, 6.5 and 8.2 wt%, respectively. By increasing sintering time to 45 min as shown in Fig. 5.13 (b), clusters of nanoparticles ostensibly reduce. Thus, smoother surface is obtained Figure 15.3 (c) shows fracture of pattern surface with 84.5 wt% Cu, 6.5 wt% and 9 wt% Ag.

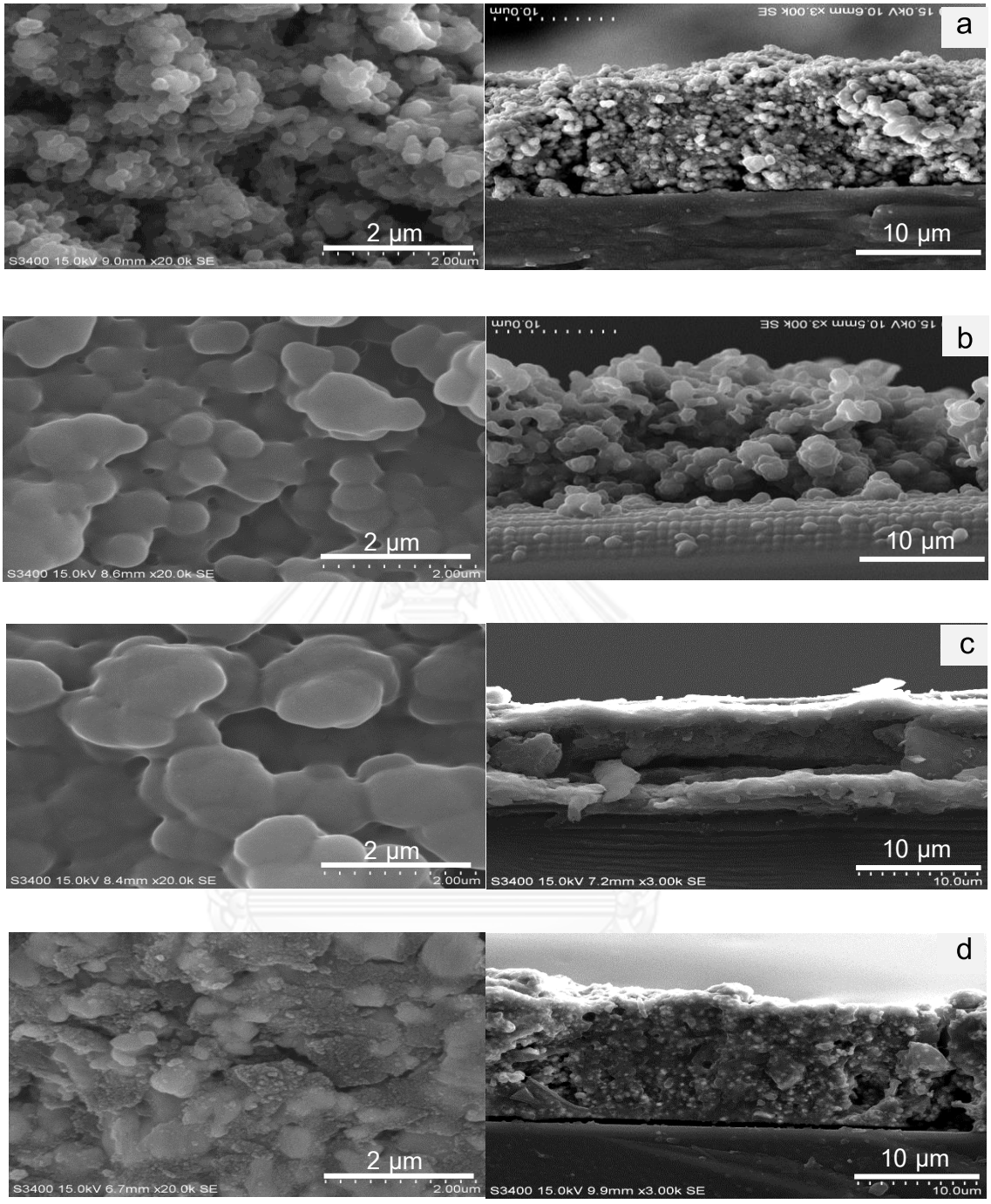

Figure 5.13 SEM and cross-section images of the printed film using nano Cu-Zn ink and then were sintered in air at 150 °C for 15 min (a), 30 min (b), 45 min (c) and 60 min (d).

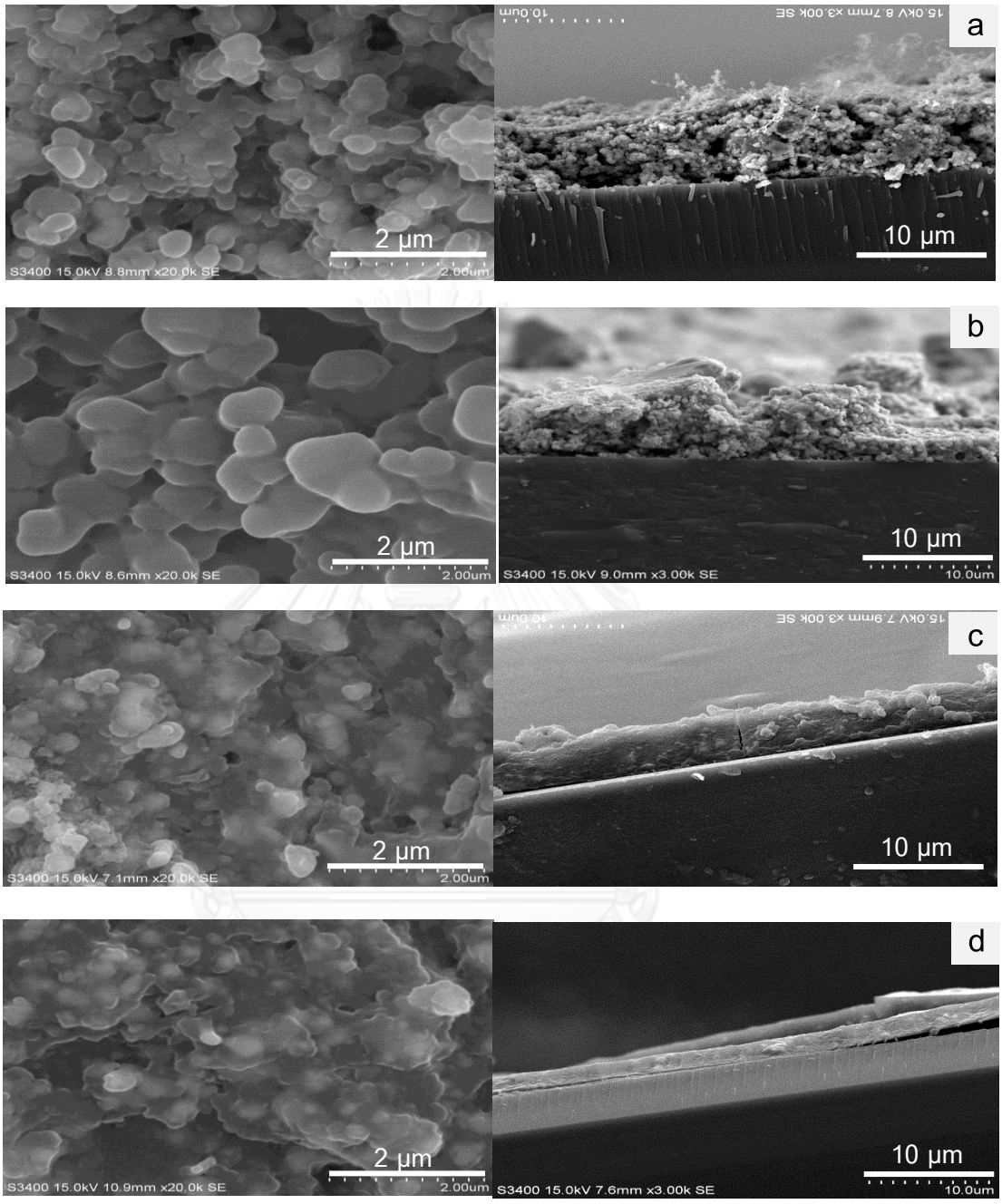

Figure 5.14 SEM and cross-section images of the printed film using nano Cu-Zn ink and then were heated in air at 100 ℃ for 30 min before sintering under 2% H_2-N_2 gas at 150 ℃ for 15 min (a), 30 min (b), 45 min (c) and 60 min (d)

.

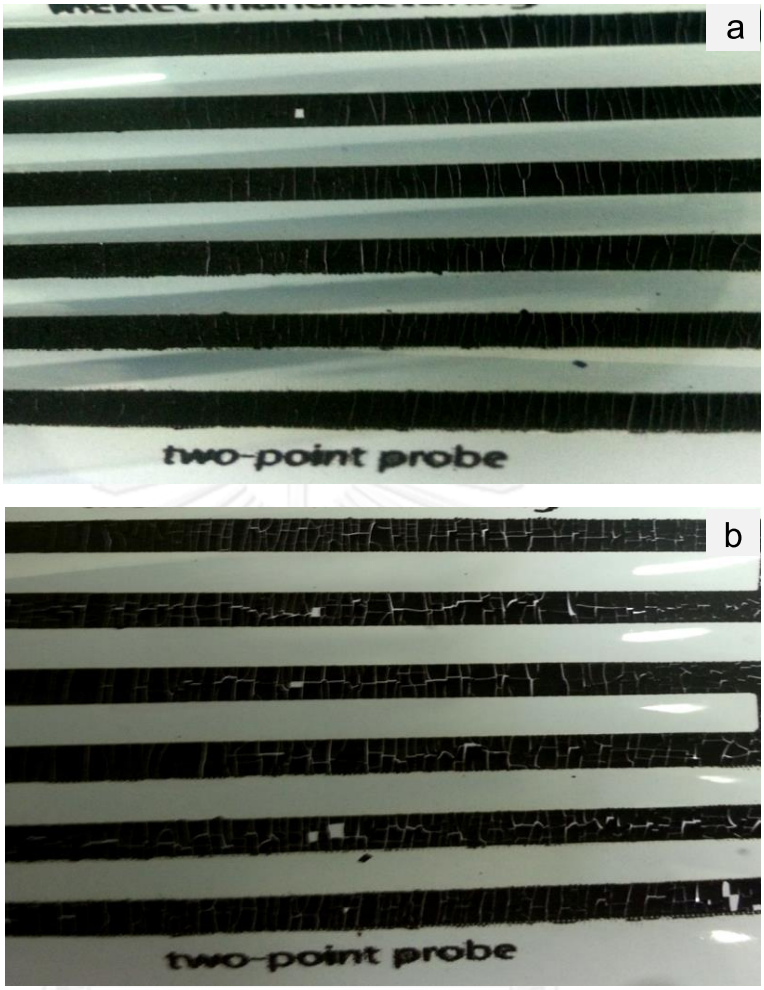

Figure 5.15 fracture of printed films was sintered for 45 min (a) and 60 min (b).

Optical images of the printed film was sintered under 2% H2-N2 mixed gas for 45 and 60 min were shown in Fig. 5.14 (a, b). Increasing of sintering time affect to more thermal expanding of PET film and Cu-Zn ink but both thermal expanding have unequal and also the ink has low adhesion. Therefore the surface of patterns has separate.

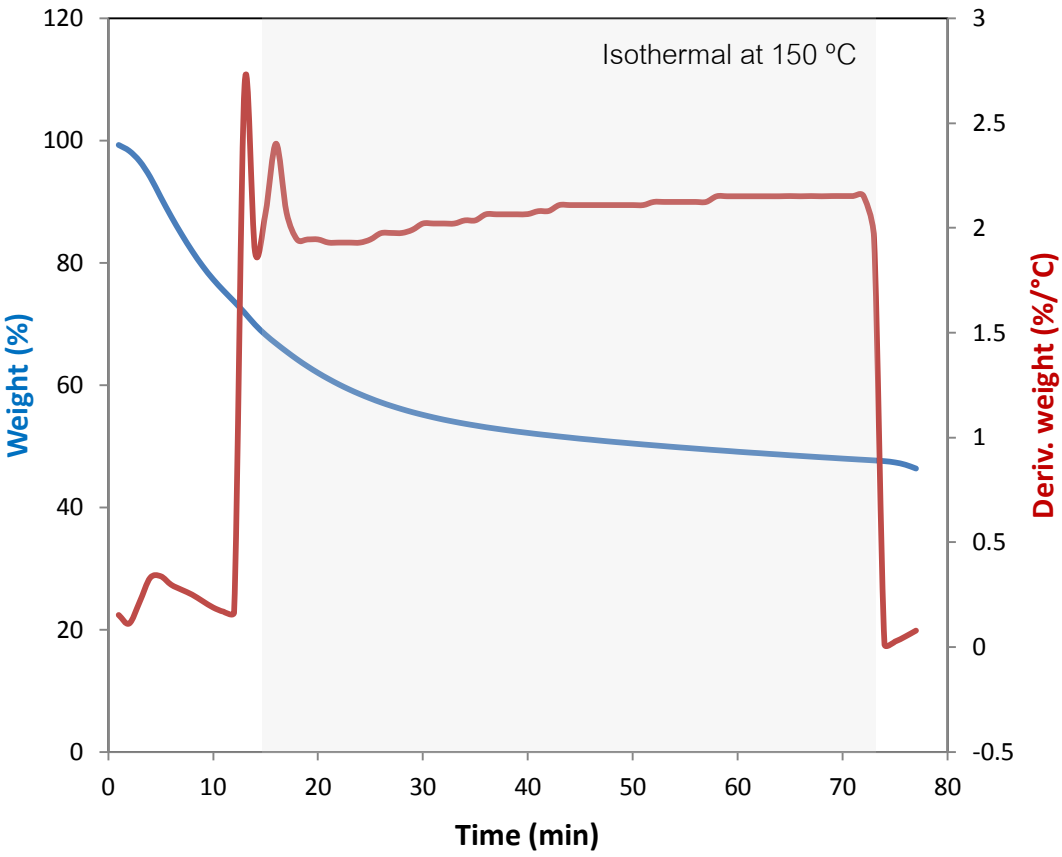

Figure 5.16 TGA/DTA curve of the Cu-Zn printed film was cured at 150 ℃ in air atmosphere.

Figure 5.15 show TGA/DTA curve of the Cu-Zn printed film was cured in air atmosphere. In beginning was heating from 24 ℃ to 150 ℃ for 15 min. This section will as rapid temperature increasing affect obviously thermal changing. For fixed temperature section at 150 ℃ since 15 min to 75 min for 60 min, was found 15% of mass loss. This loss of weight at 150 ℃ was caused by evaporation of water and organic compound.

Volume resistivity of Cu-Zn film annealed under air and 2% H_2-N_2 gas at 150 ℃ for 15, 30, 45 and 60 min are shown in table 5.1. At 0 min or before sintering could not be measured. Increasing time of film printed sintering in air to significantly increase resistivity of sintered film. Because that it more melting of silver binder and also losing of organic and water in the pattern. The lowest volume resistivity of the conductive patterns obtained by sintering time for 60 min. Thickness, width and length of printed pattern were 8 μm, 2 mm and 27 mm, respectively. These values were estimated as volume resistivity and as 190 μΩ cm for curing time to 60 min. It is 50 times of Cu90/Zn10 bulk and 108 times of copper bulk. And also, increasing time of sintering under 2% H_2-N_2 mixed gas affect higher volume resistivity. Two-step annealing was observed. In first step, oxidation in air-stable was occurred. This stage, organic compound and water are evaporated. And in second step, the surface of film was reduced in 2% H_2-N_2 mixed gas. Fracture of printed films was sintered for 45 min and 60 min was cause of do not conductivity. Therefore, the lowest volume resistivity of the printed film was 403 μΩ cm by sintering time for 15 min. At 45 min and 60 min of sintering by two steps could not conduct because its pattern is separate (Fig. 5.14). And that time, thickness of pattern to reduce form 8 μm to 5 μm expect that effect of evaporation of organic compound and reducing oxygen after bake in hydrogen. At 30 min of them, it starts separate and then has high resistivity. From result of sintering found the pattern is sintered in two steps use sintering time less than in air for produce low conductive pattern.

Table 5.1 summary of volume resistivity of the printed film under various annealing conditions.

Atmosphere		Annealing Time (min)	Film thickness (μm)	Volume resistivity (μΩ cm)
Pre-heat at 100 °C for 30 min	Annealing ambient			
-	Air	0	15	-
-	Air	15	8	5191
-	Air	30	8	2666
-	Air	45	8	1244
-	Air	60	8	190
Air	2% H_2-N_2	0	8	3496
Air	2% H_2-N_2	15	8	403
Air	2% H_2-N_2	30	8	28266
Air	2% H_2-N_2	45	5	-
Air	2% H_2-N_2	60	5	-

CHAPTER VI

CONCLUSIONS

6.1 Summary of Results

CuZn alloy nanoparticles were synthesized by submerged arc discharge method from Cu-Zn alloy wire 90Cu/10Zn. Dielectric liquid type and cooling temperature influence to chemical composition and size of nanoparticles synthesized. Cu-Zn and ZnO were formed in deionized water, ethanol and ethylene glycol. In contrast, nanoparticles synthesized in diethanolamine do not form CuO and ZnO, because diethanolamine can act as a weak reducing agent and also as a capping agent in order to protect the surface of the nanoparticles. The size of nanoparticles obtained depends on the dielectric liquid used.The smallest size of CuZn alloy nanoparticles synthesized in ethylene glycol and diethanolamine were spherical with 10-20 nm and 20-30 nm. In comparison, deionized water was the largest particles of 20–60 nm. Storing time of Cu-Zn colloid affect to particle size its. After was stored for 2 month and 6 month, the particle size were 30 nm and 95 nm, respectively. Cu-Zn colloid solution which was synthesized in diethanolamine solvent had 93 %wt of Cu and 7 %wt of Zn. Adding of silver complex solution into Cu-Zn colloid, effect to well melting at low temperature. Increasing time of film printed sintering in air to significantly increase resistivity of sintered film. That is because oxygen atoms on surface of printed pattern were continually removed. Lowest volume resistivity of printed film was 190 μΩ cm for annealing time in air to 60 min and contained Cu 82 %wt, Zn 8 %wt and Ag 10 %wt. In comparison, volume resistivity of the printed film was 403 μΩ cm by sintering time in 2% H_2-N_2 mixed gas for 15 min after pre-heat in air for 30 min. So, hydrogen is a part of reduce oxygen which adhere on the surface of the pattern. The conductive ink based on Cu-Zn nanoparticles synthesized was air-stable and can be sintered in air and hydrogen-nitrogen mixed gas at low temperature.

6.2 Recommendations

6.2.1 Do not store the nano Cu-Zn colloids in diethanolamine are long time before apply it to Cu-Zn conductive ink.

6.2.2 The effect of Cu-Zn colloid and binder ratio should be studies.

REFERENCES

1. Faddoul, R., et al., *Optimisation of silver paste for flexography printing on LTCC substrate.* Microelectronics Reliability, 2012. **52**(7): p. 1483-1491.
2. Tai, Y.L. and Z.G. Yang, *Preparation of stable aqueous conductive ink with silver nanoflakes and its application on paper-based flexible electronics.* Surface and Interface Analysis, 2012. **44**(5): p. 529-534.
3. Ahlers, M., *The martensitic transformation in the Cu–Zn based shape memory alloys as a tool for the evaluation of transformation mechanisms and phase stabilities.* Materials Science and Engineering: A, 2008. **481**: p. 500-503.
4. Tang, X.-F., Z.-G. Yang, and W.-J. Wang, *A simple way of preparing high-concentration and high-purity nano copper colloid for conductive ink in inkjet printing technology.* Colloids and Surfaces A: Physicochemical and Engineering Aspects, 2010. **360**(1): p. 99-104.
5. Kamyshny, A., J. Steinke, and S. Magdassi, *Metal-based inkjet inks for printed electronics.* Open Applied Physics Journal, 2011. **4**: p. 19-36.
6. Kassaee, M.Z., et al., *Media effects on nanobrass arc fabrications.* Journal of Alloys and Compounds, 2008. **453**(1): p. 229-232.
7. Kazakevich, P.V., et al., *Phase diagrams of laser-processed nanoparticles of brass.* Applied surface science, 2007. **253**(19): p. 7724-7728.
8. Kazakevich, P.V., et al., *Laser induced synthesis of nanoparticles in liquids.* Applied surface science, 2006. **252**(13): p. 4373-4380.
9. Wang, F., H. Gu, and Z. Zhang, *Preparation of cobalt nanocrystals in the homogenous solution with the presence of a static magnetic field.* Materials research bulletin, 2003. **38**(2): p. 347-351.
10. Kassaee, M.Z. and F. Buazar, *Al nanoparticles: impact of media and current on the arc fabrication.* Journal of manufacturing processes, 2009. **11**(1): p. 31-37.
11. Kassaee, M.Z., F. Buazar, and E. Motamedi, *Effects of current on arc fabrication of Cu nanoparticles.* Journal of Nanomaterials, 2010. **2010**: p. 7.
12. Sano, N., et al., *Study on reaction field in arc-in-water to produce carbon nano-materials.* Thin Solid Films, 2008. **516**(19): p. 6694-6698.

13. Wei, Z.-Q., et al., *Processing parameters for Cu nanopowders prepared by anodic arc plasma.* Transactions of Nonferrous Metals Society of China, 2007. **17**(1): p. 128-132.
14. Komeily-Nia, Z., M. Montazer, and M. Latifi, *Synthesis of nano copper/nylon composite using ascorbic acid and CTAB.* Colloids and Surfaces A: Physicochemical and Engineering Aspects, 2013. **439**: p. 167-175.
15. Farbod, M. and A. Mohammadian, *Single phase synthesis of γ-brass (Cu< sub> 5</sub> Zn< sub> 8</sub>) nanoparticles by electric arc discharge method and investigation of their order–disorder transition temperature.* Intermetallics, 2014. **45**: p. 1-4.
16. Lo, C.-H., T.-T. Tsung, and H.-M. Lin, *Preparation of silver nanofluid by the submerged arc nanoparticle synthesis system (SANSS).* Journal of Alloys and Compounds, 2007. **434**: p. 659-662.
17. Chen, S.-P., et al., *Silver conductive features on flexible substrates from a thermally accelerated chain reaction at low sintering temperatures.* ACS applied materials & interfaces, 2012. **4**(12): p. 7064-7068.
18. Yabuki, A. and N. Arriffin, *Electrical conductivity of copper nanoparticle thin films annealed at low temperature.* Thin Solid Films, 2010. **518**(23): p. 7033-7037.
19. Kim, J.-H. and J.-W. Park, *Improving the flexibility of large-area transparent conductive oxide electrodes on polymer substrates for flexible organic light emitting diodes by introducing surface roughness.* Organic Electronics, 2013. **14**(12): p. 3444-3452.
20. Ashkarran, A.A., *A novel method for synthesis of colloidal silver nanoparticles by arc discharge in liquid.* Current Applied Physics, 2010. **10**(6): p. 1442-1447.
21. Lei, J.P., et al., *Formation and hydrogen storage properties of< i> in situ</i> prepared Mg–Cu alloy nanoparticles by arc discharge.* international journal of hydrogen energy, 2009. **34**(19): p. 8127-8134.
22. Song, A.J., et al., *Preparation and growth of Ni–Cu alloy nanoparticles prepared by arc plasma evaporation.* Materials Letters, 2010. **64**(10): p. 1229-1231.
23. Kim, C.K., et al., *A novel method to prepare Cu@ Ag core–shell nanoparticles for printed flexible electronics.* Powder Technology, 2014. **263**: p. 1-6.
24. Lee, B., et al., *A low-cure-temperature copper nano ink for highly conductive printed electrodes.* Current Applied Physics, 2009. **9**(2): p. e157-e160.

25. Mukhopadhyay, N.K., et al., *Synthesis and characterization of nano-structured Cu–Zn γ-brass alloy.* Materials Science and Engineering: A, 2008. **485**(1): p. 673-680.
26. Tojo, C., F. Barroso, and M. de Dios, *Critical nucleus size effects on nanoparticle formation in microemulsions: A comparison study between experimental and simulation results.* Journal of colloid and interface science, 2006. **296**(2): p. 591-598.
27. Chung, Y.M., et al., *A study of pulsed plasma oxidation effects on the corrosion resistance of brass.* Surface and Coatings Technology, 2004. **188**: p. 473-477.
28. Dagher, S., et al., *Synthesis and optical properties of colloidal CuO nanoparticles.* Journal of Luminescence, 2014. **151**: p. 149-154.
29. Yu, E.-K., L. Piao, and S.-H. Kim, *Sintering Behavior of Copper Nanoparticles.* BULLETIN OF THE KOREAN CHEMICAL SOCIETY, 2011. **32**(11): p. 4099-4102.
30. Li, W. and M. Chen, *Synthesis of stable ultra-small Cu nanoparticles for direct writing flexible electronics.* Applied surface science, 2014. **290**: p. 240-245.
31. Kundrapu, M., Shashurin, A and Keidar, M, *A model of carbon nanotube synthesis in arc discharge plasmas*. JOURNAL OF PHYSICS D: APPLIED PHYSICS, 2012. **45**: p. 315305.

APPENDIX

- **Particle size calculations**

From Scherrer equation:

$$D = \frac{K\lambda}{\beta \cos\theta} \quad \text{..... (1)}$$

Where D = Crystallite size, Å

K = Crystallite-shape factor = 0.9

λ = X-ray wavelength, 1.5418 Å for CuKα

θ = Observed peak angle, degree

β = X-ray diffraction broadening, radian

Warren formula:

$$\beta = \sqrt{B_M{}^2 - B_s{}^2} \quad \text{..... (2)}$$

Where B_M = The measured peak width in radians at half peak height

B_s = The corresponding width of the standard material

The haft-height width of the diffraction peak = 0.287°

= (2π x 0.287)/360

= 0.0050 radian

The corresponding haft-height width of peak of α-alumina at the 2θ of 22.6°

=0.0038 radian

Hence, the broadening, β = $\sqrt{(0.0050^2 - 0.0038^2)}$

= 0.0033 radian

Therefore,

The crystallite size = $\frac{0.9\ x\ 1.5418\ \text{Å}}{0.0033\ x\ cos\ 11.3}$

= 430 Å = 43 nm.

VITA

Miss Neungruthai Panuthai was born on May 26th, 1990 in Bangkok, Thailand. She received the Bachelor Degree of Chemical Engineering from Mahidol University in 2011 and then entered the Master Degree of Chemical Engineering at Chulalongkorn University.